homology in both databases. As a confirmation, the rB19ECP-binding 80-kDa protein reacted with anti-Ku80 antibody (Figure 2B). Competitive ELISA further confirmed the specific binding between Ku80 and B19. Biotinylated recombinant Ku80 (rKu80) reacted with rB19ECP fixed to microwells (Figure 3A); the binding was selectively inhibited by unlabeled rKu80 but not by recombinant Ku70 (rKu70), globoside, or recombinant soluble CD26 (sCD26)[23] (Figure 3B). This binding was also inhibited in the presence of native B19 particles from infected patients (Figure 3C). Two anti-Ku80 antibodies significantly inhibited the binding of biotinylated rKu80 and rB19ECP, whereas anti-Ku70 antibody or anti-CD106 antibody failed to inhibit the binding (Figure 3D).

Ku80 participates in B19 binding and subsequent entry

We next investigated whether Ku80 would participate in B19 binding on the cell surface and facilitate B19 entry. KU812Ep6, U937, H9, and ACHN cells efficiently bound B19 (Figure 1A) and all of these cells clearly expressed Ku80 on their surface (Figure 4A). On the other hand, Ku80 was undetectable on T24, SW620, and HeLa cells, and no binding of B19 occurred (Figures 4A and 1A). An in vitro infection experiment demonstrated efficient replication of B19 DNA in KU812Ep6 cells that expressed both Ku80 and P antigen. B19 failed to amplify itself in U937, H9, and ACHN cells, which express Ku80 but no detectable levels of P antigen on the cell surface (Figures 1 and 4A). T24, SW620, and HeLa cells were nonpermissive for B19 infection although they expressed P antigen (Figure 1) and α5β1 integrin.

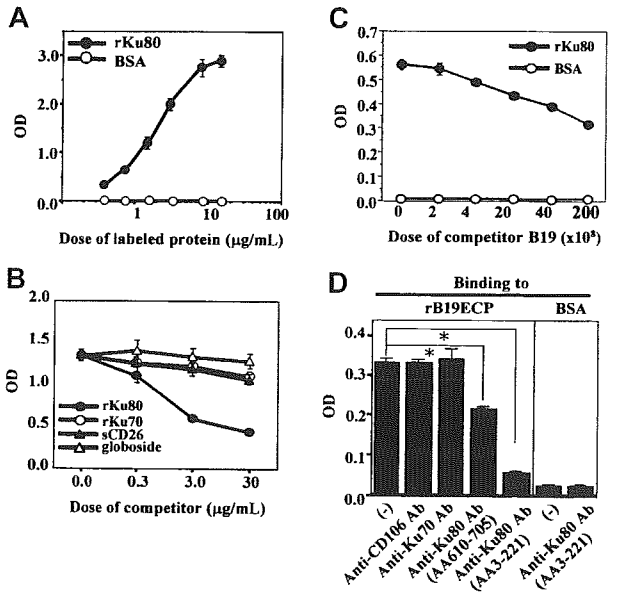

Figure 3. Specific binding of rB19ECP to Ku80. (A) Specific binding of Ku80 to rB19ECP. Indicated concentration of biotinylated rKu80 or biotinylated BSA was reacted with rB19ECP fixed to 96 microwells and detected by ELISA. (B) Competitive ELISA for rB19ECP binding to rKu80. Biotinylated rKu80 (2 μg/mL) was reacted with rB19ECP fixed to wells in the presence of indicated doses of unlabeled rKu80, rKu70, sCD26, or globoside. (C) Inhibition of rB19ECP binding to rKu80 by purified B19. Biotinylated rKu80 (1 μg/mL) was added to rB19ECP fixed to wells in the presence of B19 that was purified from B19+ serum with repeated microfiltration. Doses of B19 are expressed as copy numbers of B19 DNA. (D) Inhibition of rB19ECP binding to rKu80 by anti-Ku80 antibodies. Binding of biotinylated rKu80 or biotinylated BSA to rB19ECP fixed to wells was measured in the presence of isotype-matched mouse monoclonal antibodies as indicated.

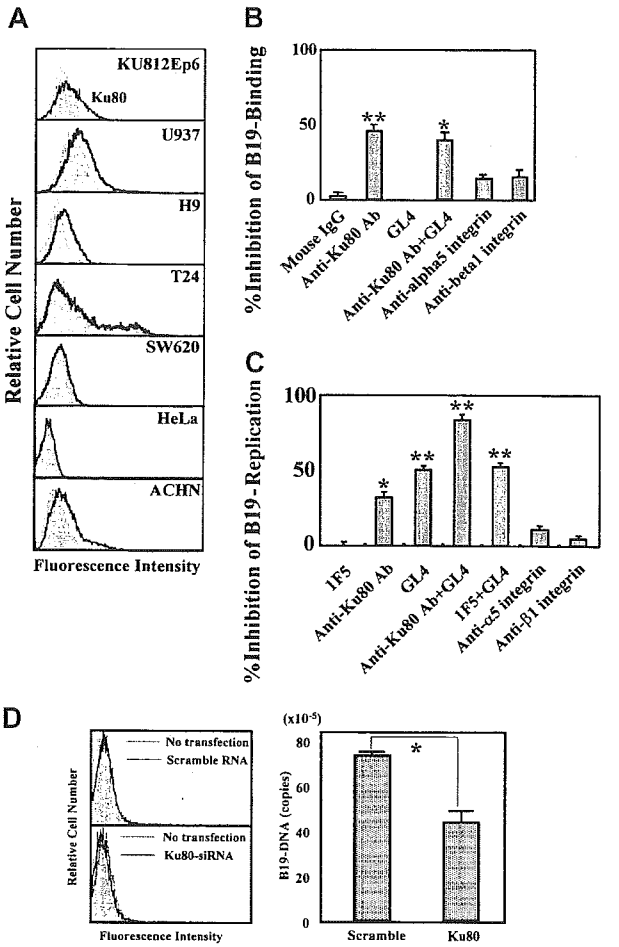

Figure 4. Role of Ku80 in B19 infection in vitro. (A) Ku80 expression on cell surface. The indicated cell lines were reacted with 5 μg/mL mouse monoclonal anti-Ku80 antibody (line) or 5 μg/mL isotype-matched mouse monoclonal antibody 1F5 (shadow), followed by FITC-labeled anti–mouse IgG antibodies. Cells were washed with PBS, and cell-surface expression of Ku80 was analyzed by flow cytometry. (B) Blocking of B19 adsorption by anti-Ku80 antibody or antiglobuside antibody. KU812Ep6 cells (2×10^6) were infected with B19 (2×10^{11} copies of B19 DNA) on ice for 30 minutes in the presence of the indicated antibodies (5 μg/mL) and extensively washed with PBS 3 times. To activate α5β1 integrin, anti-integrin antibodies were used in the presence of divalent ions (1 mM Mn^{2+}, 1 mM Mg^{2+}). B19 DNA in each group was quantified by quantitative PCR. The blocking ability of B19 binding by each antibody was expressed as percent decrease of B19-DNA in each group compared to that in antibody-untreated cells. $^{**}P < .01$, $^{*}P < .05$ by Student *t* test. (C) Blocking of B19 replication by anti-Ku80 antibody or antigloboside antibody. KU812Ep6 cells were infected with B19 and washed as described. Cells were further incubated for 48 hours at 37°C and washed with PBS 3 times before the quantitative study of B19 DNA. To activate α5β1 integrin, anti-integrin antibodies were used in the presence of divalent ions (1 mM Mn^{2+}, 1 mM Mg^{2+}). The blocking ability of B19 replication by each antibody was expressed as described. $^{**}P < .01$, $^{*}P < .05$ by Student *t* test. (D) RNA interference of Ku80 in KU812Ep6 cells. Cell-surface expression of Ku80 was examined by flow cytometry in scramble RNA or siRNA of Ku80-transfected KU812Ep6 cells (left panel). KU812Ep6 cells treated with indicated RNA were reacted with 5 μg/mL mouse monoclonal anti-Ku80 antibody or 5 μg/mL isotype-matched mouse monoclonal antibody 1F5 (shadow), followed by FITC-labeled anti–mouse IgG antibodies. B19 association of siRNA-transfected KU812Ep6 cells was evaluated by quantitative PCR (right panel). Sample DNA was prepared from extensively washed scramble RNA or siRNA of Ku80-transfected KU812Ep6 cells after 2 hours of incubation with B19. $^{*}P < .01$ by Student *t* test.

Ku80 functions as a coreceptor for B19 infection together with P antigen

We then performed an inhibition test for B19 infection of KU812Ep6 cells using antibodies against Ku80, P antigen, α5β1 integrin. Anti-Ku80 antibody inhibited B19 binding, whereas anti-P antibody, GL4, did not inhibit B19 binding. Anti–α5 and anti–β1

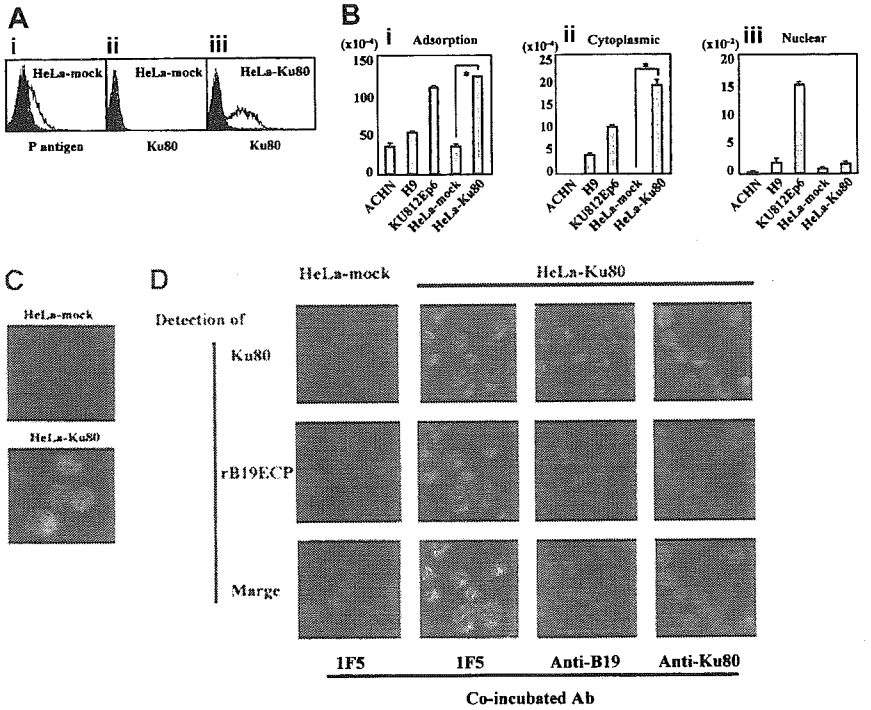

Figure 5. Transfection of Ku80 to HeLa cells. (A) Expression of Ku80 on HeLa cells transfected with pKu80. Ku80 cDNA was inserted to expression plasmid pcD and the resulted pKu80 was transfected to HeLa cells (HeLa-Ku80) using lipofectin. Empty pcD was used for a mock transfection (HeLa-mock). The transfected cells (2×10^5) were incubated with 5 μg/mL of each antibody, anti-Ku80 antibody (ii,iii), GL4 (A1), or isotype-matched mouse monoclonal antibodies or rabbit serum (shadow), and then analyzed for the expression of P antigen or Ku80 on the cell surface. Figures show HeLa-mock expressed P antigen but not Ku antigen on the surface (i,ii), whereas HeLa-Ku80 expressed Ku80 (iii). (B) Increased binding and viral entry of B19 in HeLa-Ku80. The indicated cells (6×10^5) were infected with B19 (2×10^{11} copies of B19 DNA) for 30 minutes on ice. After washing cells 3 times with PBS, pH 7.2, DNA was extracted from 2×10^5 cells. Remaining cells were further incubated for 30 minutes at 37°C. After washing cells 3 times with PBS, pH 4.5, a cytoplasmic and nuclear fraction was prepared, and then DNA was extracted from each fraction. Prepared DNA was subjected to a quantitative PCR to quantify B19 DNA. $^*P < .01$ by Student *t* test. (C) B19 infection to HeLa-Ku80. HeLa-mock or HeLa-Ku80 cells (2×10^5) were infected with B19 (2×10^{11} copies of B19 DNA) for 30 minutes at 37°C. After being washed 3 times with PBS, cells were collected with 5 mM EDTA-PBS, pH 7.2, fixed with 4% paraformaldehyde and reacted with PAR3, followed by FITC-labeled anti–mouse IgG antibody as a secondary antibody. Thus prepared cells were then subjected to a confocal microscope analysis. The panel represents B19 entered into HeLa-Ku80. (D) Colocalization of rB19ECP and Ku80. HeLa-mock or HeLa-Ku80 (2×10^5) cells were incubated with biotinylated rB19ECP (1 μg/mL) in the presence of 5 μg/mL inhibitor antibody indicated for 30 minutes at 37°C. After being washed 3 times with PBS, pH 7.2, cells were collected with 5 mM EDTA-PBS, and rB19ECP or Ku80 was detected by confocal microscopy analysis. Ku80 was detected by anti-Ku80 antibody followed by TRITC-labeled anti–mouse IgG antibody as a secondary antibody. Detection of biotinylated rB19ECP was done by avidin-FITC as described in "Materials and methods."

integrin antibodies caused a slight inhibition of B19 binding (Figure 4B). Both anti-Ku80 antibody and GL4 also inhibited B19 replication in KU812Ep6 cells. The simultaneous presence of both antibodies more strongly inhibited the replication of B19 DNA (Figure 4C). Presence of anti–α5 and anti–β1 integrin antibodies caused only a slight inhibition of B19 replication (Figure 4C). In other experiments, KU812Ep6 cells were treated with siRNA against Ku80 and then tested for the replication of B19 at B19 infection study. The results revealed the suppression of B19 binding to the KU812Ep6 cells with reduced expression of Ku80 (Figure 4D).

The role of Ku80 as a coreceptor for B19 infection was also supported by a transfection experiment using HeLa cells that were nonpermissive for B19 infection. Figure 5A shows that the surface of Ku80-transfected HeLa cells (HeLa-Ku80) became positive for Ku80 expression and binding of B19 to the cells was significantly enhanced (Figure 5B). Quantitative analysis of B19 DNA (Figure 5B) and confocal laser microscopy (Figure 5C) confirmed that B19 DNA and B19 protein were present in the cytoplasmic fraction of HeLa-Ku80 cells 30 minutes after infection, similar to Ku812Ep6. Furthermore, a coincubation experiment of rB19ECP and HeLa-Ku80 revealed the colocalization of rB19ECP and Ku80 in the cytoplasm or membrane (or both) of HeLa-Ku80 (Figure 5D). Moreover, association of rB19ECP and HeLa-Ku80 was apparently inhibited by the presence of anti-B19 antibody or anti-Ku80 antibody (Figure 5D).

Ku80 is expressed on the surface of bone marrow cells

Because Ku80 is known as a nuclear protein, it is important to determine whether or not Ku80 is expressed on the cell-surface in vivo. Ku80 was not detected on the cell surface of peripheral blood mononuclear cells (data not shown). We then examined cell-surface expression of Ku80 in bone marrow cells because bone marrow cells are potential targets of B19 infection. Flow cytometry analysis of bone marrow cells demonstrated that Ku80 was highly expressed on the cell surface of erythroid progenitor cells expressing glycophorin A as well as on the surface of immune cells such as $CD20^+$, $CD3^+$, or $CD14^+$ cells in bone marrow (Figure 6A). A small portion (5.6%) of $CD36^+$ bone marrow cells, which may be permissive to B19 infection,[23] were also positive for the expression of Ku80 on the cell surface (Figure 6B). B19 binding to bone marrow cells was inhibited in the presence of anti-Ku80 antibody at B19 infection in vitro (data not shown). Figure 7 shows that the replication of B19 in bone marrow cells was significantly inhibited in the presence of anti-Ku80 antibody or GL4. The inhibition rate of B19 replication in the presence of both anti-Ku80 antibody and GL4 was similar to that in the presence of GL4.

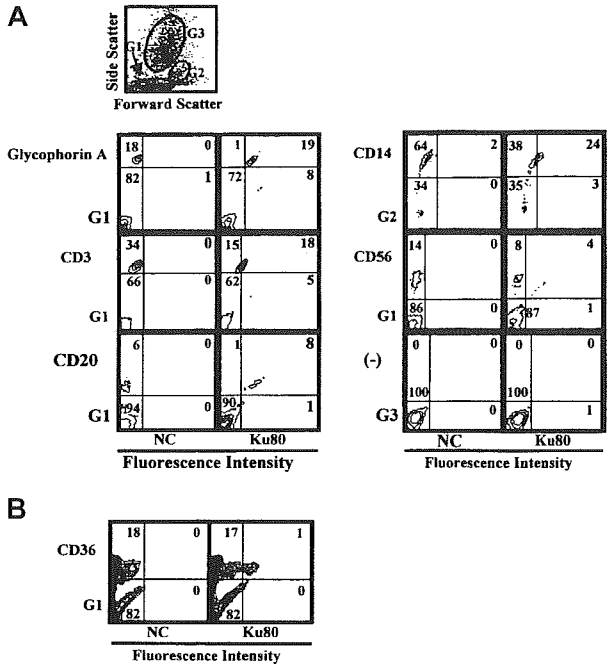

Figure 6. Cell-surface expression of Ku80 in human bone marrow cells. Flow cytometry analysis of Ku80 expression on the cell surface. Bone marrow cells were reacted with indicated antibodies and anti-Ku80 antibody as described in "Materials and methods," and then the expression of surface molecules was analyzed. Prior to the study, each sample had been analyzed by the scattered plot. The results showed that the glycophorin A^+, $CD3^+$, $CD20^+$, $CD56^+$, or $CD36^+$ cells were scattered in gate 1 (G1), and $CD14^+$ cells in gate 2 (G2), and that there were no glycophorin A^+, $CD3^+$, $CD20^+$, $CD56^+$, or $CD36^+$ cells in gate 3 (G3). Then the expression of Ku80 on cell surface in gated cells was analyzed. The gate used in each experiment is shown at left-lower side of each plot. (A) Gates used in the experiment and detection of Ku80 on the surface of various cell lineages. (B) Detection of Ku80 on the surface of $CD36^+$ bone marrow cells.

Discussion

The presented data implicate Ku80 as a coreceptor involved in B19 infection. U937, H9, and ACHN cells expressing Ku80 showed B19 binding, but some cells with P antigen failed to bind B19 unless these cells expressed Ku80 on their surface. A marked increase in B19 binding in Ku80-transfected HeLa cells and the inhibition of B19 infectivity by anti-Ku80 antibody or siRNA to Ku80 suggests a Ku80-dependent B19 interaction with the targeted cells. Specific inhibition of B19 binding by anti-Ku80 antibody that recognized the N-terminus of the Ku80 protein suggests that B19 interacts with specific sites of Ku80 on the cell surface. Further, Epstein-Barr virus or hepatitis virus C failed to bind either to Ku80-expressing HeLa or U937 cells (data not shown). These results suggest that Ku80 is one of the specific receptors for B19 infection.

Ku is a heterodimeric DNA-binding protein consisting of a 70-kDa (Ku70) and an 80-kDa (Ku80) subunit and was originally identified as a nuclear antigen recognized by autoantibodies in patients with systemic lupus erythematosus and scleroderma.[25] Ku has a central role in multiple nuclear processes, including DNA repair, chromosome maintenance, transcription regulation, and V(D)J recombination. Ku is abundant in the nucleus, consistent with its function as a DNA-protein kinase (DNA-PK).[26,27] However, recent studies have shown cytoplasm or surface localization of Ku in various types of cells, including of leukemia, multiple myeloma, and tumor cell lines. Ku is a component of the DNA-PK complex in membrane rafts of mammalian cells.[26] Although the role of surface Ku80 has not been well clarified,[28] signal transduction and Ku80 are coupled in both B and T cells,[25,28,29] and localization of the DNA-PK complex in lipid rafts suggests a putative role in the signal transduction pathway following ionizing radiation.[26] It was recently reported that Ku interacts with metalloproteinase 9 at the cell surface of highly invasive hematopoietic cells of normal and tumor cell origin, and Ku80/MMP-9 interaction at the cell membrane may result in contribution to the invasion of tumor cells through regulation of extracellular matrix remodelling.[30] Further, the membrane form of Ku, whose expression is induced at hypoxia, mediates cell adhesion of plasma cells,[30-32] indicating a role for Ku as an adhesion receptor for fibronectin.[33] The present study showed that Ku80 is positive on the surface of $CD3^+$ cells, $CD20^+$ cells, $CD14^+$ cells, glycophorin A^+ cells, and $CD36^+$ cells from bone marrow where B19 infection is permissive.

We have discovered a novel role of Ku80 as a cellular receptor in B19 infection. Anti-Ku80 antibody, however, did not cause complete inhibition of B19 infection, whereas pretreatment with anti-Ku80 antibody together with GL4 strongly inhibited B19 infectivity in KU812Ep6 cells and human bone marrow cells, showing the necessity of P antigen as a receptor. A recent report showed that α5β1 integrin has a role in B19 entry into host cells,[6] and KU812Ep6, U937, H9, ACHN, and HeLa cells all expressed α5β1 integrin on their surface (data not shown). However, B19 entry into U937- and H9-expressing Ku80 and α5β1 integrin or HeLa cells with P antigen and α5β1 integrin was insufficient or negative (Figures 1 and 5B). B19 entry was marked in KU812Ep6 cells or Ku80-HeLa cells that expressed Ku80, P antigen, and α5β1 integrin on their surface, showing the necessity of P antigen for efficient binding and the virus entry afterward. Anti–α5 and anti–β1 integrin antibodies, which inhibited the entry of B19 into K562 cells,[6] caused a slight inhibition of B19 binding as well as B19 replication in KU812Ep6, supporting the participation of α5β1 integrin in B19 infection. We are currently investigating the precise mechanism of the interaction among B19-related receptors such as P antigen, Ku80, and α5β1 integrin in association with the following signal transduction in B19-infected cells.

The use of multiple receptors for entry into cells has been observed frequently in virus infection, such as by α herpesviruses, HHV-8 or HIV.[34,35] We have shown that B19 uses at least 2 receptors, Ku80 and P antigen, in the process of infection. Ku80

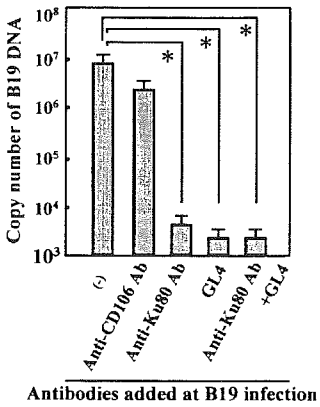

Figure 7. Blocking of B19 infection of bone marrow cells by anti-Ku80 antibody or antiglobloside antibody. Bone marrow cells (2×10^6) were infected with B19 (2×10^{11} copies of B19 DNA) with the indicated antibodies and evaluated for quantity of B19 DNA as described. Anti-CD106 antibody was a mouse monoclonal antibody used as a negative control. The differences in the results between control (−) and other samples were statistically analyzed. $^*P < .01$ by Student *t* test.

may function as an efficient B19-capturing molecule on the cell surface and may also contribute to B19 entry into cells; markedly enhanced entry of B19 in Ku80-HeLa cells (Figure 5C-D) suggests that Ku80 mediates efficient B19 entry in cooperation with P antigen and probably with α5β1 integrin.[6] Although Ku80 can interact with Epstein-Barr virus protein in the nucleus,[36] this study is the first to show the use of Ku80 antigen as a cellular receptor for virus infection. Despite marked entry of B19, synthesis of B19 protein was unsuccessful in Ku80-HeLa cells, but was possible only in erythroid cell lines, indicating that unknown intracellular factors may be required for B19 replication in the targeted cells.[37,38]

Ku80 is not found in circulating mononuclear cells from healthy volunteers but is positive on the surface of B19-binding cells in vivo, such as immune cells in tonsils, erythroblasts, T cells, B cells, macrophages in bone marrow, and immune cells including follicular dendritic cells in rheumatoid joints, indicating the surface expression of Ku antigen may be restricted by environmental conditions. Of interest is that the oxygen levels are markedly low in bone marrow and joints[39-41] compared with that in blood, and surface Ku80 is inducible with hypoxia.[31,32] A recent study suggests the efficiency of B19 infection increases with hypoxia.[42] These studies suggest that surface Ku80 induced with hypoxia may participate in the process of B19 infection of joints and bone marrow.

Ku80 expression on the surface of immune cells in bone marrow in vivo may explain clinical findings associated with B19 infection to nonerythroid cells. Namely, B19 infection often causes a decreased number of leukocytes or lymphocytes in blood during acute B19 infection, as well as increased levels of TNF-α and IFN-γ in blood or rheumatoid joints, and the detection of B19 on T cells, B cells, or macrophages in tonsils, bone marrow, or rheumatoid joints. B19 may infect immune cells in bone marrow or the synovium and persist to lead to secrete an inflammatory cytokine through the activation of AP1 and AP2 by B19 NS1.[43] Stimulation of cellular receptors with B19 may trigger activation of signal cascades in host cells, which may explain why immune cells in acute and prolonged B19 infection or in the joints of rheumatoid arthritis are functionally altered.

Acknowledgments

We are grateful to E. Miyagawa for KU812Ep6, K. Kamata for rB19ECP, T. Mimori for rKu80 and rKu70, C. Morimoto for sCD26, K. Yamaguchi for purified B19, and S. Shibahara for the pKu80.

References

1. Anderson MJ, Jones SE, Fisher-Hoch SP, et al. Human parvovirus, the cause of erythema infectiosum (fifth disease) [letter]? Lancet. 1983;1:1387.
2. Brown KE, Young NS. Parvovirus B19 in human disease. Annu Rev Med. 1997;48:59-67.
3. Brown KE, Anderson SM, Young NS. Erythrocyte P antigen: cellular receptor for B19 parvovirus. Science. 1993;262:114-117.
4. Weigel-Kelly KA, Yoder MC, Srivastava A. Recombinant human parvovirus B19 vectors: erythrocyte P antigen is necessary but not sufficient for successful transduction of human hematopoietic cells. J Virol. 2001;75:4110-4116.
5. Kaufmann B, Baxa U, Chipman PR, Rossmann MG, Modrow S, Seckler R. Parvovirus B19 does not bind to membrane-associated globoside in vitro. Virology. 2005;332:189-198.
6. Weigel-Kelley KA, Yoder MC, Srivastava A. α5β1 integrin as a cellular co-receptor for human parvovirus B19: requirement of functional activation of {beta} 1 integrin for viral entry. Blood. 2003; 102:3927-3933.
7. Wagner AD, Goronzy JJ, Matteson EL, Weyand CM. Systemic monocyte and T cell activation in a patient with human parvovirus B19 infection. Mayo Clin Proc. 1995;70:261-265.
8. Murai C, Munakata Y, Takahashi Y, et al. Rheumatoid arthritis after human parvovirus B19 infection. Ann Rheum Dis. 1999;58:130-132.
9. Anderson MJ, Higgins PG, Davis LR, et al. Experimental parvovirus infection in humans. J Infect Dis. 1985;152:257-265.
10. Barlow GD, Mckendrick MW. Parvovirus B19 causing leucopenia and neutropenia in a healthy adult. J Infect. 2000;40:192-195.
11. Nesher G, Osborn TG, Moore TL. Parvovirus infection mimicking systemic lupus erythematosus. Semin Arthritis Rheum. 1995;24:297-303.
12. Kerr JR, Barah F, Mattey DL, et al. Circulating tumor necrosis factor-α and interferon-γ are detectable during acute and convalent parvovirus B19 infection and are associated with prolonged and chronic fatigue. J Gen Virol. 2001;82:3011-3019.
13. Soderlund M. Persistence of parvovirus B19 DNA in synovial membranes of young patients with and without chronic arthropathy. Lancet. 1997; 349:1063-1065.
14. Takahashi Y, Murai C, Munakata Y, et al. Human parvovirus B19 as a causative agent for rheumatoid arthritis. Proc Natl Acad Sci U S A. 1998;95: 8227-8232.
15. Miyagawa E, Yoshida T, Takahashi H, et al. Infection of the erythroid cell line, KU812Ep6 with human parvovirus B19 and its application to titration of B19 infectivity. J Virol Methods. 1999;83:45-54.
16. Saito T, Munakata Y, Fu Y, et al. Evaluation of anti-parvovirus B19 activity in sera by assay using quantitative polymerase chain reaction. J Virol Methods. 2003;107:81-87.
17. Yamaguchi K, Miyagawa E, Dan M, Miyazaki T, Ikeda H. Cellulose hollowfibers (BMMS) used in the filter membrane can trap human parvovirus B19 [abstract]. Electron Microsc. 2002;2:115.
18. Kajigaya S, Shimada T, Fujita S, Young NS. Self-assembled B19 parvovirus capsids, produced in a baculovirus system, are antigenically and immunogenically similar to native virions. Proc Natl Acad Sci U S A. 1991;88:4646-4650.
19. Yaegashi N, Tada K, Shiraishi H, Ishii T, Nagata K, Sugamura K. Characterization of monoclonal antibodies against human parvovirus B19. Microbiol Immunol. 1989;33:561-567.
20. Brown CS, Jensen T, Meloen RH, et al. Localization of an immunodominant domain on baculovirus produced parvovirus B19 capsids: correlation to a major surface region on the native virus particle. J Virol. 1992;66:6989-6996.
21. Harata N, Sasaki T, Osaki H, et al. Therapeutic treatment of New Zealand mouse disease by a limited number of anti-idiotypic antibodies conjugated with neocarzinostatin. J Clin Invest. 1990; 86:769-776.
22. Okayama H, Berg P. A cDNA cloning vector that permits expression of cDNA inserts in mammalian cells. Mol Cell Biol. 1983;3:280-289.
23. Tanaka T, Duke-Cohen JS, Kameoka J, et al. Enhancement of antigen-induced T-cell proliferation by soluble CD26/dispetidyl peptidase IV. Proc Natl Acad Sci U S A. 1994;91:3082-3086.
24. Morey AL, Fleming KA. Immunophenotyping of fetal haematopoietic cells permissive for human parvovirus B19 replication in vitro. Br J Haematol. 1992;82:302-309.
25. Mimori T, Ohosone Y, Hama N, et al. Isolation and characterization of cDNA encoding the 80-kDa subunit protein of the human autoantigen Ku(p70/p80) recognized by autoantibodies from patients with scleroderma-polymyositis overlap syndrome. Proc Natl Acad Sci U S A. 1990;87: 1777-1781.
26. Adam L, Bandyopadhyay D, Kumar R. Interferon-α signaling promotes nucleus-to-cytoplasmic redistribution of p95Vav, and formation of a multisubunit complex involving Vav, Ku80, and Trk-2. Biochem Biophys Res Commun. 2000;267:692-696.
27. Hector L, Darren G, Guillermo ET. Novel localization of the DNA-PK complex in lipid rafts. J Biol Chem. 2003;278:22136-22143.
28. Prabhakar BS, Allaway GP, Srinivasappa J, Notkins AL. Cell surface expression of the 70-kD component of Ku, a DNA-binding nuclear autoantigen. J Clin Invest. 1990;86:1301-1305.
29. Morio T, Hanissian SH, Bacharier LB, et al. Ku in the cytoplasm associates with CD40 in human B cells and translocates into the nucleus following incubation with IL-4 and anti-CD40 mAb. Immunity. 1999;11:339-348.
30. Monferran S, Paupert J, Dauvillier S, Salles B, Muller C. The membrane form of the DNA repair protein Ku interacts at the cell surface with metalloproteinase 9. EMBO J. 2004;23:3758-3768.
31. Teoh G, Urashima M, Greenfield EA, et al. The 86-kD subunit of Ku autoantigen mediates homotypic and heterotypic adhesion of multiple myeloma cells. J Clin Invest. 1998;101:1379-1388.
32. Lynch EM, Moreland RB, Ginis I, Perrine SP, Faller DV. Hypoxia-activated ligand HAL1/13 is lupus autoantigen Ku80 and mediates lymphoid cell adhesion in vitro. Am J Physiol Cell Physiol. 2001;280:897-911.
33. Sylvie M, Catherine M, Lionel M, Philippe F, Bernard S. The membrane-associated form of the DNA repair protein Ku is involved in cell

adhesion to fibronectin. J Mol Biol. 2004;26: 503-511.

34. Spear PG, Eisenberg RJ, Cohen GH. Three classes of cell surface receptors for alphaherpesvirus entry. Virology. 2000;275:1-8.
35. Shaw MA, Naranatt PP, Fu ZW, Bala C. Integrin α3β1(CD49c/29) is a cellular receptor for Kaposi's sarcoma-associated herpesvirus (KSHV/HHV-8) entry into the T cells. Cell. 2002;108:407-419.
36. Shieh B, Schultz J, Guinness M, Lacy J. Regulation of the human IgE receptor (Fc epsilonRII/CD23) by Epstein-Barr virus (EBV): Ku autoantigen binds specifically to an EBV-responsive enhancer of CD23. Int Immunol. 1997;9:1885-1895.
37. Liu JM, Green SW, Shimada T, Young NS. A block in full-length transcript maturation in cells nonpermissive for B19 parvovirus. J Virol. 1992;66: 4686-4692.
38. Brunstein J, Soderlund VM, Hedman K. Identification of a novel splicing pattern as a basis of restricted tropism of erythrovirus B19. Virology. 2000;274: 284-291.
39. Bodamyali T, Stevens CR, Billingham MEJ, Ohta S, Blake DR. Influence of hypoxia in inflammatory synovitis. Ann Rheum Dis. 1998;57: 703-710.
40. Harrison SJ, Rameshwer P, Chang V, Bandari P. Oxygen saturation in the bone marrow of healthy volunteers [letter]. Blood. 2002;99:394.
41. Cemanec J, Guilak F, Weinberg JB, Piestsky DS, Fermor B. Influence of hypoxia and reoxygenation on cytokine-induced production of proinflammatory mediators in articular cartilage. Arthritis Rheum. 2002;46:968-975.
42. Piellet S, Guyader NL, Hofer T, et al. Hypoxia enhances human B19 erythrovirus gene expression in primary erythroid cells. Virology. 2004;327:1-7.
43. Fu Y, Ishii KK, Munakata Y, Saito T, Kaku M, Sasaki T. Regulation of tumor necrosis factor α promoter by human parvovirus B19 NS1 through activation of AP1 and AP2. J Virol. 2002;76:5359-5365.

A *CCR2-V64I* polymorphism affects stability of CCR2A isoform

Emi E. Nakayama, Yuetsu Tanaka,[a] Yoshiyuki Nagai,[b] Aikichi Iwamoto[c] and Tatsuo Shioda

Objective: A valine to isoleucine substitution at position 64 of CCR2 (*CCR2-64I*) is associated with a delay in progression to AIDS in HIV-1-infected individuals. The aim of the present study is to elucidate the molecular mechanism underlying the effect of this allele.

Design: We analysed the effect of the 64I substitution on levels of expression of CCR2A and CCR2B, two CCR2 isoforms produced by alternative splicing.

Methods: Sendai virus vector was used to express CCR2 molecules.

Results: While CCR2B trafficked well to the cell surface, CCR2A, which differs from CCR2B only by the sequence of its C-terminal cytoplasmic tail, was detected predominantly in the cytoplasm. The level of expression of CCR2A-64I was significantly higher than that of CCR2A without the substitution. On the other hand, the 64I substitution did not affect levels of CCR2B expression. Pulse–chase experiments revealed that the 64I substitution increased the half-life of CCR2A in cells. When co-expressed with CCR5, CCR2A-64I interfered more severely with cell surface expression of CCR5 than did wild-type CCR2A. Furthermore, immunoprecipitation experiments showed that CCR2A co-precipitated with an immature form of CCR5.

Conclusion: These results suggest that CCR2A binds to CCR5 in the cytoplasm and down-modulates its surface expression. We propose that the increased ability of CCR2A-64I to down-modulate CCR5 expression might be a possible cause of a delay in HIV-1 disease progression in patients with this allele.

AIDS 2004, **18**:729–738

Keywords: polymorphism, CCR2-64I, CCR2A, CCR5, stability

Introduction

The chemokine receptor CCR2B has been regarded as a minor HIV-1 coreceptor because only a small number of HIV-1 strains has been shown to use CCR2B as an entry coreceptor [1–3]. Nevertheless, a polymorphism in the CCR2 gene, *CCR2-64I*, has been reported to be associated with delayed disease progression in HIV-1 infected individuals in several Caucasian cohorts [4–8]. This polymorphism, a G-to-A transition at position 190, changes CCR2B codon 64 from valine to isoleucine, introducing a conservative amino acid change into the first transmembrane domain. It was unclear why a single amino acid substitution in a minor coreceptor could affect HIV-1 disease progression, as there was no difference in HIV-1 co-receptor activity between the variant CCR2B-64I and CCR2B without the 64I substitution (CCR2B-64V) [9,10]. Furthermore, these studies also excluded the possibility that CCR2B-64I exerts a dominant-negative effect on the expression and activity of CCR5.

From the Research Institute for Microbial diseases, Osaka University, Osaka, the [a]University of the Ryukyus, Okinawa, [b]Toyama Institute of Health, Toyama, and the [c]Institute of Medical Science, University of Tokyo, Tokyo, Japan.

Correspondence to T. Shioda, Department of Viral Infections, Research Institute for Microbial Diseases, Osaka University. 3-1 Yamada-oka, Suita-shi, Osaka 565-0871, Japan.

Received: 5 May 2003; revised: 27 September 2003; accepted: 15 October 2003.

DOI: 10.1097/01.aids.0000111407.02002.15

ISSN 0269-9370 © 2004 Lippincott Williams & Wilkins

It is possible that the *CCR2* polymorphism may be linked to other polymorphisms in genes that influence AIDS progression. The *CCR2* gene is located approximately 15 kb from the 5′ end of the *CCR5* gene, and the *CCR2-64I* allele is indeed linked to a certain *CCR5* promoter haplotype [11]. However, experiments using promoter–reporter fusion constructs showed that the *CCR5* promoter haplotype, which is in a strong linkage disequilibrium with *CCR2-64I*, did not affect transcriptional activity of the *CCR5* promoter [10]. Thus, the mechanism underlying the protective effect of *CCR2-64I* against AIDS progression still remained to be elucidated.

Two alternatively spliced CCR2 isoforms, CCR2A and CCR2B, were reported to be present in freshly isolated human monocyte, THP-1, and MonoMac 6 leukaemia cell lines [12,13]. An open reading frame encoded in the chromosome corresponds to CCR2B, while alternatively spliced transcripts produce CCR2A. The two CCR2 isoforms differ only in their C-terminal cytoplasmic tails (Fig. 1). Therefore, an individual carrying the *CCR2-64I* allele also produces CCR2A molecules with isoleucine at position 64. Although the cytoplasmic tail spans less than one-fifth of the entire CCR2 molecule, this difference caused a drastic alteration in their localization in cells [13]. While CCR2B trafficked well to the cell surface, CCR2A was detected predominantly in the cytoplasm. A progressive truncation study of the C-terminal cytoplasmic tail indicated that a cytoplasmic retention signal(s) was located in the C-terminal cytoplasmic tail [13]. Nevertheless, CCR2A molecules that successfully trafficked to the cell surface could respond to the stimulation of monocyte chemoattractant protein (MCP)-1 in a similar fashion to CCR2B [14].

As none of the previous studies investigated the effect

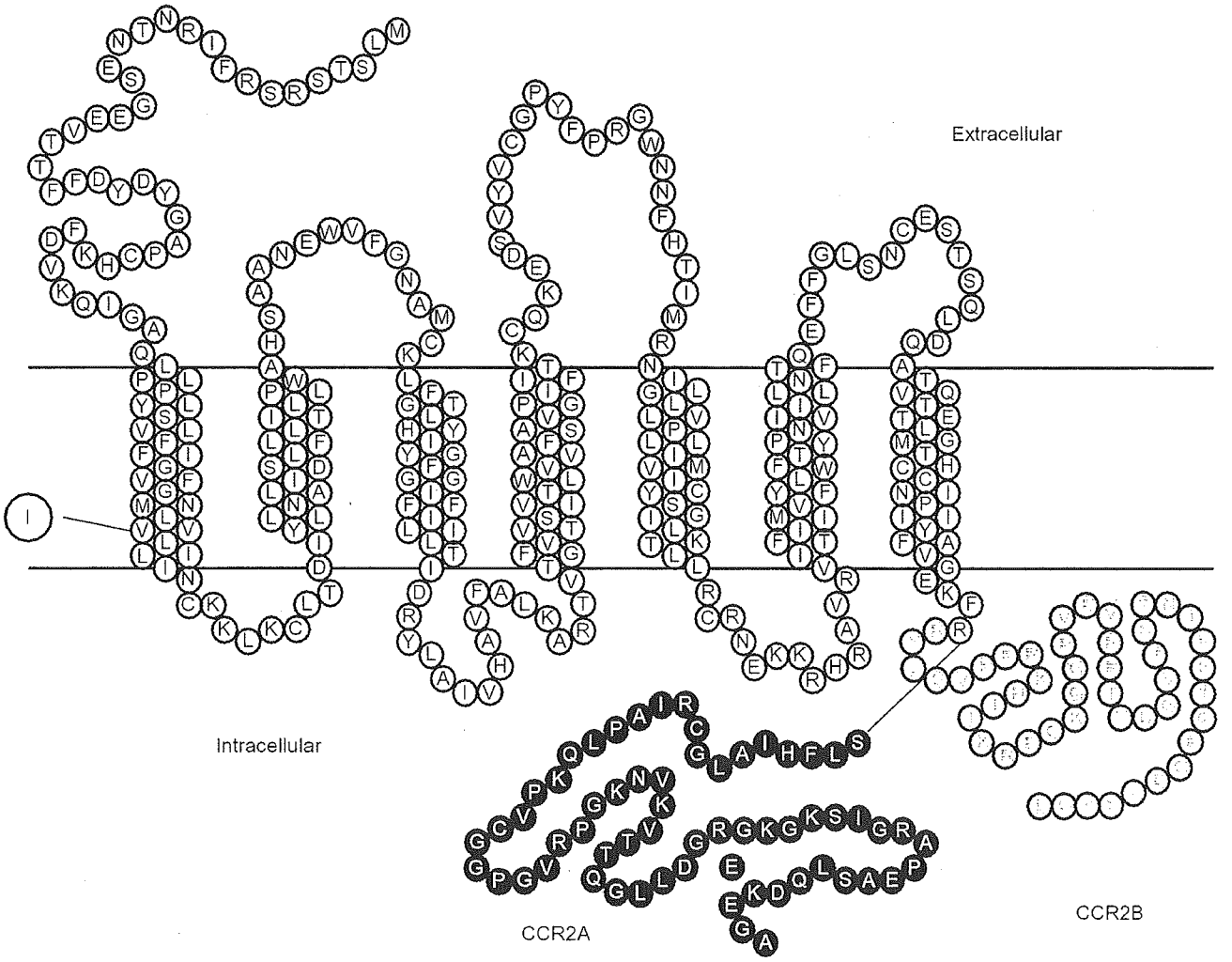

Fig. 1. The structure of the CCR2A and CCR2B molecules. Outlined letters in grey circles denote amino acid residues present in CCR2B. Outlined letters in black circles denote amino acid residues present in CCR2A. A letter I in a large circle denotes a substitution at position 64.

of the 64I substitution on CCR2A molecules, we generated recombinant Sendai viruses (SeV) expressing either CCR2A-64V or CCR2A-64I. Here we show that the 64I substitution indeed affected the stability of CCR2A molecules in cells, and increased the ability of CCR2A to down-modulate the major HIV-1 co-receptor, CCR5.

Materials and methods

Generation of recombinant SeV

THP-1 cells were shown to possess both *CCR2-64V* and *CCR2-64I* alleles by using a standard genotyping method [15]. Therefore, CCR2A-64V, CCR2A-64I, CCR2B-64V, and CCR2B-64I cDNA were obtained by reverse transcription (RT)–PCR from mRNA extracted from THP-1 cells and then inserted to the *Not*I site of pSeV18+b(+). The entire coding regions in the resultant plasmids were verified for sequence authenticity as well as for the presence or absence of the 64I substitution. For generating CCR2A-64V and CCR2A-64I cDNA carrying a c-myc-tag (EQKLI SEEDL) at their C-termini, cloned CCR2A-64V and CCR2A-64I cDNA served as templates for PCR amplification using a primer containing a nucleotide sequence corresponding the c-myc-tag fused with the C-terminal portion of CCR2A. Recombinant SeV carrying CCR2A-64V, CCR2A-64I, CCR2B-64V, CCR2B-64I, or C-myc-tagged versions of CCR2A-64V and CCR2A-64I were recovered according to a previously described method [16]. The wild-type Z strain of SeV served as a control in all the experiments.

Generation of a recombinant vaccinia virus

For generating CCR5 cDNA carrying a HA tag (YPYDVPDYAA) at its C terminus, cloned CCR5 cDNA served as a template for PCR amplification by using a primer containing a haemagglutinin (HA) tag sequence fused with the C-terminal portion of CCR5. The resultant PCR products were then inserted into pNZ68K2-Not. The entire coding region of CCR5-HA was verified for sequence authenticity. A recombinant vaccinia virus (Vac) was recovered from the resultant plasmid according to previously described procedures [17].

Flow cytometric analysis

CV1 monkey kidney cells, U937 monocytic cells and Jurkat T cells were infected with recombinant SeV expressing CCR2A-64V, CCR2A-64I, CCR2B-64V, or CCR2B-64I. Five to 18 h after infection, cells were incubated with MAB150, a mouse monoclonal antibody (MAb) against CCR2 (R & D Systems, Minneapolis, Minnesota, USA). Antibodies bound to cells were detected using fluorescein-5-isothiocyanate (FITC)-conjugated goat antibody directed against mouse IgG (Cappel, Aurora, Ohio, USA). CV1 or H9 cells infected with SeV expressing CCR2A-64V, CCR2A-64I, CCR2B-64V, or CCR2B-64I were superinfected with a recombinant Vac expressing CCR5, CXCR4, or CD4 at 9 h after SeV infection. After incubation for 5 h at 37°C, cells were stained for CCR5 using T227 rat MAb against CCR5 [17] followed by FITC-conjugated goat anti-rat IgG; for CXCR4 using 12G5 mouse MAb (R & D systems) followed by FITC-conjugated goat anti-mouse IgG; or for CD4 using FITC-conjugated anti-human CD4, Leu3a (Becton Dickinson, San Jose, California, USA), and analysed by FACScan (Becton Dickinson).

Immunofluorescence microscopy

CV1 cells expressing CCR2A or CCR2B were fixed and permeabilized before being incubated with MAB150 antibody as described previously [17]. Bound antibodies were then detected using FITC-conjugated goat antibody against mouse IgG. Indirect immunofluorescence was visualized using a Lasersharp2000 Confocal Microscope System (Bio-Rad, Hercules, California, USA). Anti-Calnexin (Stressgen, San Diego, California, USA) or anti-Giantin (CRPinc, Berkeley, California, USA) rabbit polyclonal antibody was used with Cy5-conjugated goat antibody against rabbit IgG (Amersham Pharmacia Biotech, Piscataway, New Jersey, USA).

Chemotaxis assay

Chemotaxis assays were performed according to previously described methods [18]. Briefly, MCP-1 (PeproTech, Rockey Hill, New Jersey, USA) diluted at an indicated concentration of chemotaxis buffer (RPMI 1640 with 0.25% human serum albumin) was added to the bottom chamber of a 5- m pore polycarbonate Transwell culture insert (Costar; Corning, New York, USA). Jurkat cells were infected with a SeV expressing CCR2A-64V or CCR2A-64I and incubated at 37°C for 4 h. Cells were then washed with RPMI1640 and re-suspended in chemotaxis buffer and added to the upper chamber of the insert. Transmigrated cells in 4 h at 37°C were counted using a FACScan.

Pulse-chase analyses of CCR2A and CCR5

CV1 or U937 cells were infected with a SeV expressing CCR2A-64V-myc or CCR2A-64I-myc. Nine hours after infection, cells were labelled with 500 kbq/ml of EXPRE^{35}S^{35}S[^{35}S] protein labelling mix (> 37 Tbq/mmol; PerkinElmer (Boston, Massachusetts, USA) in amino acid-free medium for 30 min. For CCR5 analysis, cells were infected with a recombinant Vac expressing CCR5-HA, incubated at 37°C for 5 h and then labelled. Cells were then washed, fed with fresh medium and incubated for 0, 15, 30, 60, or 120 min at 37°C, chilled on ice, and lysed in lysis buffer (50 mM Tris–HCl pH7.5, 150 mM NaCl, 1% Nonidet P40, 0.5% sodium deoxycholate). CCR2A

and CCR5 proteins in the lysates were precipitated with anti-myc mouse MAb (9B11; Cell Signaling, Beverly, Massachusetts, USA) and anti-HA high affinity rat MAb (Roche, Indianapolis, Indiana, USA), respectively, using a Protein G Immunoprecipitation Kit (Roche). Precipitated materials were subjected to SDS–PAGE on a 4–12% NuPAGE Bis–Tris gel (Invitrogen, Groningen, Netherlands), and the amount of radiolabel incorporated was visualized on a BAS Imager (Fujix, Kanagawa, Japan).

Gene reporter fusion assay

A recombinant Vac-based gene activation assay using a -galactosidase gene as a reporter was performed as described previously [19]. Briefly, mouse fibroblast L cells were transfected with -galactosidase reporter plasmid pGINT7 -gal and infected with a recombinant Vac expressing gp160 of an R5 HIV-1 strain SF162. At the same time, CV1 cells were infected with SeV expressing CCR2A-64V or CCR2A-64I and incubated at 37°C for 9 h. Cells were then superinfected with recombinant Vacs expressing T7 RNA polymerase, human CD4, and CCR5, detached by trypsinization, and cultured at 37°C for 5 h. Then, L and CV-1cells were mixed, incubated for 3 h, and -galactosidase activities in the cell lysate were measured by using chlorophenol red- -D-galactopyranoside as substrate.

HIV-1 productive infection

MT4 cells (4×10^5) were infected with SeV expressing CCR2A-64V, CCR2A-64I or parental Z strain of SeV at a multiplicity of infection (MOI) of 40 plaque forming unit (PFU)/cell mixed with SeV expressing CCR5 at an MOI of 10 PFU/cell and incubated at 37°C for 5 h. Cells were then superinfected with 60 ng p24 of an R5 HIV-1 strain SF162. The culture supernatants were collected periodically and p24 levels were measured.

Immunoprecipitation and western blot analysis

CV1 cells were infected with SeV expressing CCR2A-64V-myc or CCR2A-64I-myc, and incubated at 37°C for 9 h. Cells were then superinfected with a Vac expressing CCR5-HA and incubated at 37°C for 5 h and then lysed. CCR2A-64V-myc, CCR2A-64I-myc or CCR5-HA proteins were immunoprecipitated, and subjected to SDS–PAGE as described above. Proteins were then electrophoretically transferred to a PVDF membrane (Immobilon; Millipore, Bedford, Massachusetts, USA). Blots were blocked and probed with the antibodies overnight at 4°C and then incubated with peroxidase-conjugated anti-mouse (Kirkegaard & Perry Laboratories, Gaithersbug, Maryland, USA) or anti-rat IgG (American Qualex, San Clemente, California, USA) and developed using the Immun-Star HRP chemiluminescent kit (Bio-Rad).

Results

Expression of CCR2A and CCR2B

We generated a recombinant SeV expressing either CCR2A-64V or CCR2B-64V. Confocal microscopic observations (Fig. 2a) and flow cytometric analyses (Fig. 2b) confirmed the different subcellular localization of these two CCR2 isoforms. In CCR2B-64V expressing CV1 cells, fluorescent signals of CCR2 were observed mainly on the cell surface. In contrast, CCR2A-64V was localized predominantly to the cytoplasm, although a small portion of CCR2A was observed on the cell surface. In the cytoplasm, signals of an endoplasmic reticulum marker calnexin were only partially co-localized with CCR2A signals (Fig. 2a, left), whereas the majority of signals for the Golgi marker giantin overlapped with those of CCR2A (Fig. 2a, right). These results suggested that most CCR2A molecules were retained in the Golgi.

To assess the effect of the 64I substitution on CCR2A expression, we generated a recombinant SeV expressing CCR2A-64I and compared levels of expression of CCR2A-64I with those of CCR2A-64V. As shown in Fig. 2b, CCR2A-64I showed slightly but significantly higher levels of expression than CCR2A-64V in various cell types, despite the same promoter being used. The mean fluorescence intensity (MFI) of CCR2A-64I and CCR2A-64V was 274 and 140 in CV1, 133 and 40 in U937 monocystic cells, and 29 and 21 in Jurkat T cells. The difference was greater in U937 cells than in Jurkat cells. The difference was also observed at 5, 12, and 18 h after infection of recombinant SeVs (Fig. 2c). Exactly the same result was obtained when recombinant SeV expressing C-myc-tagged versions of CCR2A-64V (CCR2A-64V-myc) and CCR2A-64I (CCR2A-64I-myc) were used (Fig. 2c). In contrast, we failed to detect any difference in the levels of expression between CCR2B-64V and CCR2B-64I (MFI 2698 and 2663, respectively; Fig. 2b), as had been described in the previous reports [9,10]. Northern blot analyses confirmed that there was no difference in the amount of CCR2 mRNA among cells expressing CCR2A-64V, CCR2A-64I, CCR2A-64V-myc, CCR2A-64I-myc, CCR2B-64V and CCR2B-64I (data not shown). These data clearly indicate that the substitution of valine to isoleucine affects levels of cell surface expression of CCR2A, but not of CCR2B.

Chemokine receptor activity of recombinant CCR2A-64V and CCR2A-64I

To determine whether or not CCR2A molecules expressed by a recombinant SeV fully retained chemokine receptor activity, we performed a chemotaxis assay. As shown in Fig. 2d, both cells expressing CCR2A-64V and CCR2A-64I migrate toward MCP-1. However, cells expressing CCR2A-64I migrated

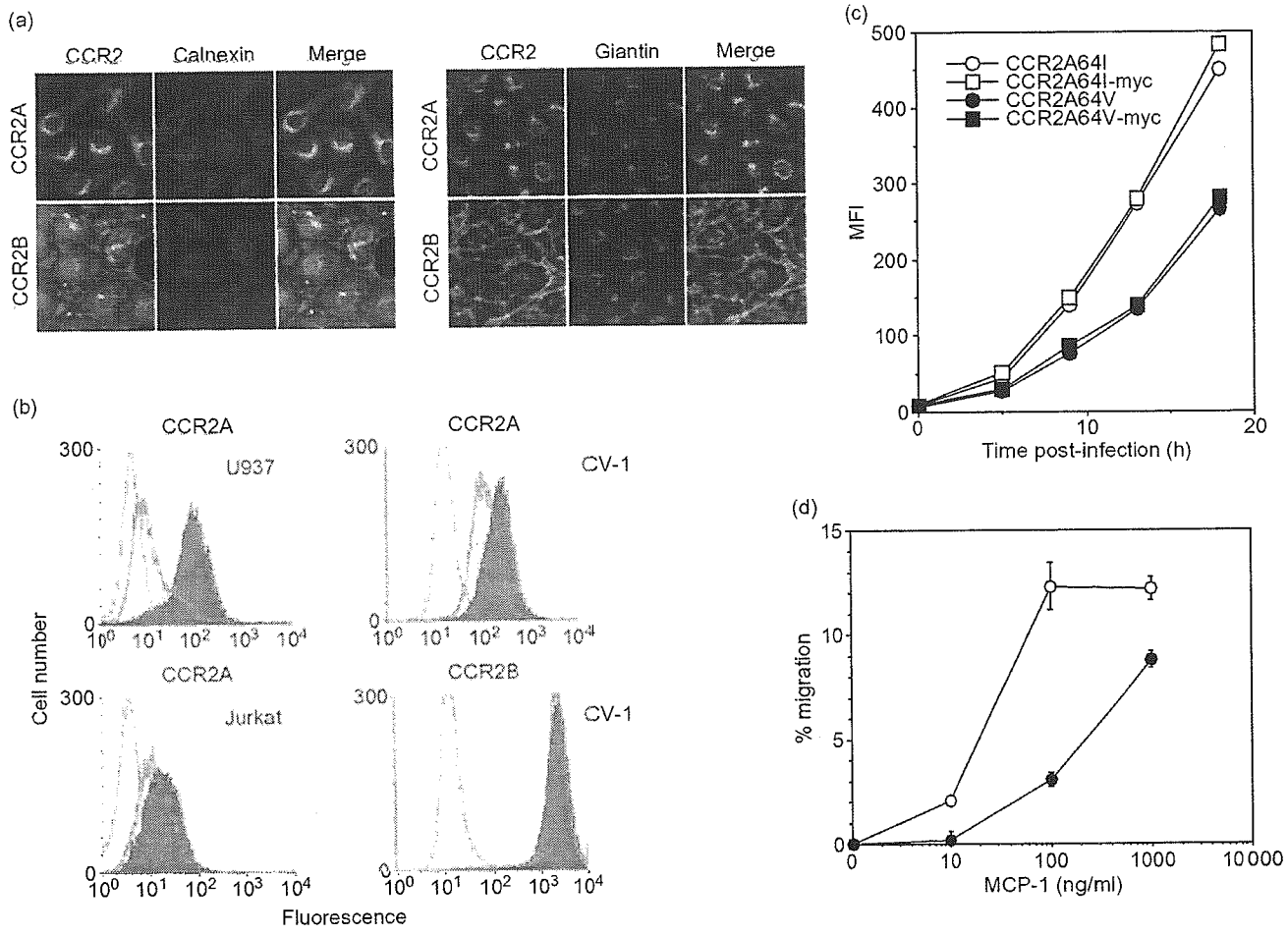

Fig. 2. (a) Subcellular distribution of CCR2A-64V and CCR2B-64V in CV1 cells. SeV vector (SeV) was used to express the CCR2A-64V and CCR2B-64V molecules. Cells were fixed and permeabilized before staining with MAB150 anti-CCR2 mouse MAb followed by FITC-labelled anti-mouse IgG. Cells were then re-stained with anti-calnexin or anti-giantin rabbit polyclonal antibody followed by Cy5-labelled anti-rabbit IgG, and analysed by confocal laser microscopy. (b) Surface expression of CCR2A-64V (green) and CCR2A-64I (red) in U937, CV1 or Jurkat cells. Cells infected with the parental Z strain served as a negative control (black). In lower right panel, green and red indicates CCR2B-64V and CCR2B-64I, respectively. (c) The cell surface expression of CCR2A-64I (open circles), CCR2A-64I-myc (open squares), CCR2A-64V (filled circles), and CCR2A-64V-myc (filled squares) at 5, 9, 12 and 18 h after infection by SeV. MFI indicates mean fluorescence intensity of each sample. (d) Chemokine receptor activity of recombinant CCR2A-64V and CCR2A-64I. Jurkat cells infected with SeV expressing CCR2A-64V (closed circles) or CCR2A-64I (open circles) migrated in response to increasing concentration of MCP-1. Data points are means of triplicate determination with standard deviations.

more efficiently than those expressing CCR2A-64V. These results are in good agreement with the observation that expression of CCR2A-64I is higher than that of CCR2A-64V.

CCR2A-64I is more stable than CCR2A-64V

Differential levels of expression between CCR2A-64V and CCR2A-64I prompted us to compare the rate of degradation of those proteins in pulse–chase experiments. For this purpose, we used recombinant SeV expressing CCR2A-64V-myc or CCR2A-64I-myc. Comparison of immunoprecipitated materials from ^{35}S-labelled CV1 cells expressing CCR2A-64V-myc and CCR2A-64I-myc showed that almost identical levels of CCR2A-64V-myc and CCR2A-64I-myc proteins were synthesized during the 30-min labelling period ($t = 0$) (Fig. 3a). However, CCR2A-64V-myc proteins appeared to degrade more rapidly than CCR2A-64I-myc proteins. The half-life of CCR2A-64I-myc was approximately 90 min, whereas that of CCR2A-64V-myc was approximately 50 min in CV1 cells (Fig. 3b). More prominent results were obtained when we used U937 cells, as the half-life of CCR2A-64I-myc was approximately 60 min, whereas that of CCR2A-64V-myc was approximately 18 min in U937 cells. This finding is in a good agreement with the observation

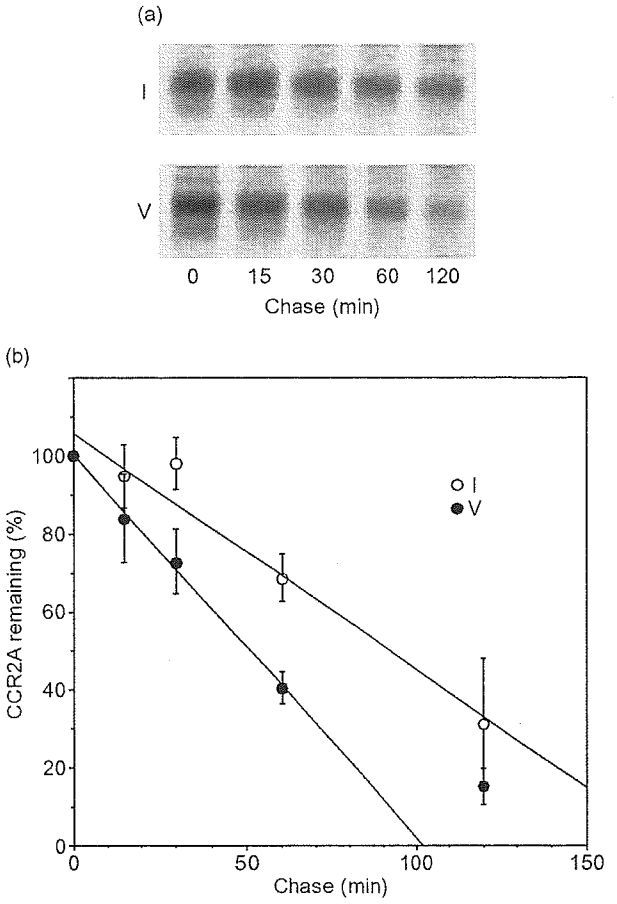

Fig. 3. CCR2A-64I is more stable than CCR2A-64V. CV1 cells were infected with SeV expressing CCR2A-64V-myc and CCR2A-64I-myc for 9 h. Cells were labelled for 30 min and then harvested following the chase time indicated. (a) Representative gels of pulse–chase analysis. (b) PhosphorImager analysis of the gels shown in (a). Open and closed circles denote cells infected with SeV expressing CCR2A-64V-myc and CCR2A-64I-myc, respectively. Data points are means of four independent experiments with standard deviations.

that the difference in cell surface expression levels between CCR2A-64V and CCR2A-64I was greater in U937 cells than in CV-1 cells (Fig. 2b). These results indicate that higher cell surface expression of CCR2A-64I was due to increased stability of CCR2A-64I. On the other hand, we failed to detect any significant difference in the half-life between CCR2B-64V and CCR2B-64I (data not shown).

CCR5 but not CXCR4 expression was more severely blocked by co-expression of CCR2A-64I than by co-expression of CCR2A-64V

To determine whether or not CCR2A has a dominant-negative effect on the expression of major HIV-1 receptor molecules, we first inoculated SeV expressing CCR2A-64V or CCR2A-64I in CV1 cells and incubated the cells for 9 h at 37°C. The cells were then superinfected with recombinant Vac expressing CCR5, CXCR4, or CD4. Five hours after Vac infection, surface expression of CCR5, CXCR4, or CD4 were examined by flow cytometry. As shown in Fig. 4a, the CCR5 MFI of cells co-infected with parental Z strain of SeV was 391, while that of the cells co-infected with SeV expressing CCR2A-64V was 297, indicating that co-expression of CCR2A-64V significantly reduced levels of CCR5 expression on the cell surface. This dominant-negative effect on CCR5 expression was more prominent when SeV expressing CCR2A-64I were used (MFI, 145) than SeV expressing CCR2A-64V were used. The same results were obtained when we used recombinant SeV expressing CCR2A-64V-myc and CCR2A-64I-myc (MFI, 300 and 179, respectively). Similar results were obtained when CV1 cells were inoculated with Vac expressing CCR5 5 h after infection by SeV expressing CCR2A, as the CCR5 MFI on cells co-infected with Z, SeV expressing CCR2A-64V, and Sev expressing CCR2A-64I, was 299, 205, and 160, respectively. Furthermore, the dominant-negative effect of CCR2A on CCR5 expression was also observed when T cell line H9 was used. The CCR5 MFI on H9 cells co-infected with Z, SeV expressing CCR2A-64V, and SeV expressing CCR2A-64I was 263, 230 and 195, respectively. In contrast, the cell surface expression of CXCR4, another major co-receptor, as well as that of CD4, the main receptor of HIV-1, were not affected by CCR2A-64V or CCR2A-64I (Fig. 4a). In contrast with CCR2A, neither CCR2B-64V nor CCR2B-64I affected the surface expression of CCR5 (Fig. 4b).

HIV-1 coreceptor activity of CCR5 was more dramatically reduced by co-expression of CCR2A-64I than by co-expression of CCR2A-64V

To assess the effect of CCR2A-64I on HIV-1 infection, we examined the ability of cells expressing both CCR2A and CCR5 molecules to support CD4-dependent cell fusion mediated by an HIV-1 envelope protein of the R5 strain SF162. For this purpose, we prepared CV1 cells expressing both CCR5 and CCR2A as described in Fig. 4a, and mixed those cells with mouse L cells expressing HIV-1 envelope protein. As shown in Fig. 5a, the envelope-mediated cell fusion activity of CCR5 was more dramatically reduced by co-expression of CCR2A-64I than by that of CCR2A-64V.

We also inoculated a live SF162 strain of HIV-1 into CD4 positive MT4 cells expressing both CCR5 and CCR2A. As shown in Fig. 5b, MT4 cells expressing CCR5 and CCR2A-64V supported SF162 replication better than those expressing CCR5 and CCR2A-64I.

Co-immunoprecipitation of CCR2A and CCR5

Many seven-transmembrane receptors, including che-

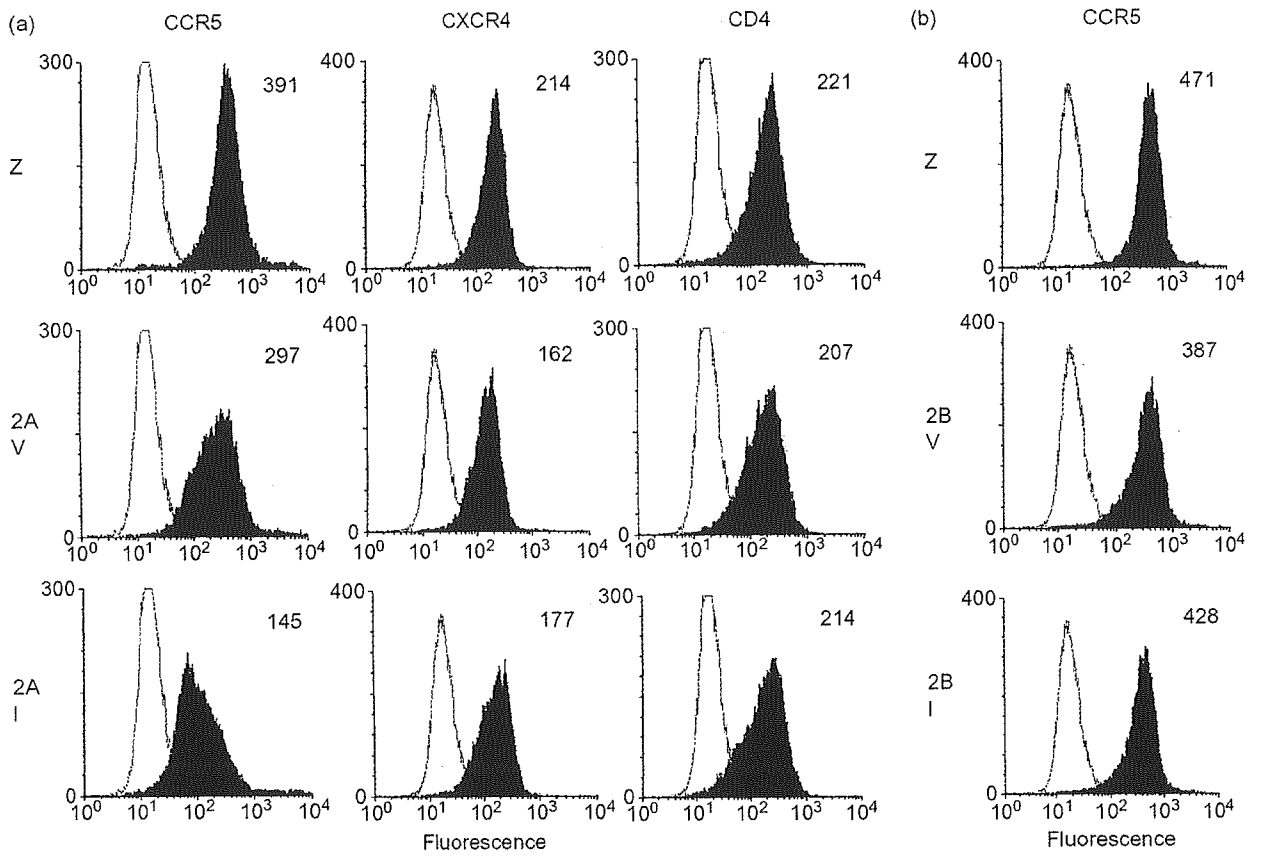

Fig. 4. (a) Effect of CCR2A-64V and CCR2A-64I on HIV-1 corecepter expression. Vac vectors were used to express CCR5, CXCR4 and CD4 in the CV1 cells inoculated with SeV expressing CCR2A-64V or CCR2A-64I. Z denotes the wild-type SeV. Five hours after infection, cells were stained with MAb against CCR5, CXCR4, or CD4. Flow cytometry was used to determine surface expression levels. The number in each panel indicates mean fluorescence intensity. (b) Effect of CCR2B-64V and CCR2B-64I on CCR5 expression.

mokine receptors, have been reported to form homo-oligomers. CCR2A is highly homologous to CCR5 (68% at the amino acid level), and formation of heterodimers between CCR2B and CCR5 was reported previously [20]. The dominant-negative effect of CCR2A on CCR5 expression shown in Figs 4a, 5a and 5b raised the possibility of heterodimer formation between CCR2A and CCR5. To test this hypothesis, we used SeV expressing CCR2A-64V-myc or CCR2A-64I-myc, and Vac expressing HA-tagged version of CCR5 (CCR5-HA). Anti-myc and anti-HA immunoprecipitates from cell lysates were developed in Western blots by using anti-HA or anti-myc antibodies. As expected, CCR5-HA was detected by anti-HA antibody in anti-myc-derived immunoprecipitates from CCR5-HA and CCR2A-64V-myc co-expressed cell lysates as well as from CCR5-HA and CCR2A-64I-myc co-expressed cell lysates. At the same time, CCR2A-64V-myc and CCR2A-64I-myc were detected by anti-myc antibody in anti-HA-derived immunoprecipitates of CCR5-HA and CCR2A-64V-myc co-expressed cell lysates and in that of CCR5-HA and CCR2A-64I-myc co-expressed cell lysates (Fig. 5c). These results clearly indicate that CCR2A formed heterodimers with CCR5.

In CCR5-HA expressing cells, we consistently observed two types of CCR5-HA molecules with different electrophoretic mobility. When we used anti-HA antibody to precipitate CCR5-HA directly, most of the CCR5-HA molecules migrated at approximately 38 kDa. In contrast, most of the CCR5-HA molecules that co-precipitated with CCR2A-64V-myc or CCR2A-64I-myc migrated at 37 kDa. We speculated that the CCR5-HA of 38 kDa represented authentic CCR5 molecules and that of 37 kDa represented immature forms of CCR5. To verify the maturation process of CCR5, we labelled the cells infected with Vac expressing CCR5-HA by [^{35}S]-methionine for 30 min and harvested those cells following chase periods ranging from 15 to 60 min. As shown in Fig. 5d, the 37-kDa CCR5-HA could be detected only after the labelling period (0 min). This result suggests that CCR2A binds to premature forms of CCR5 and

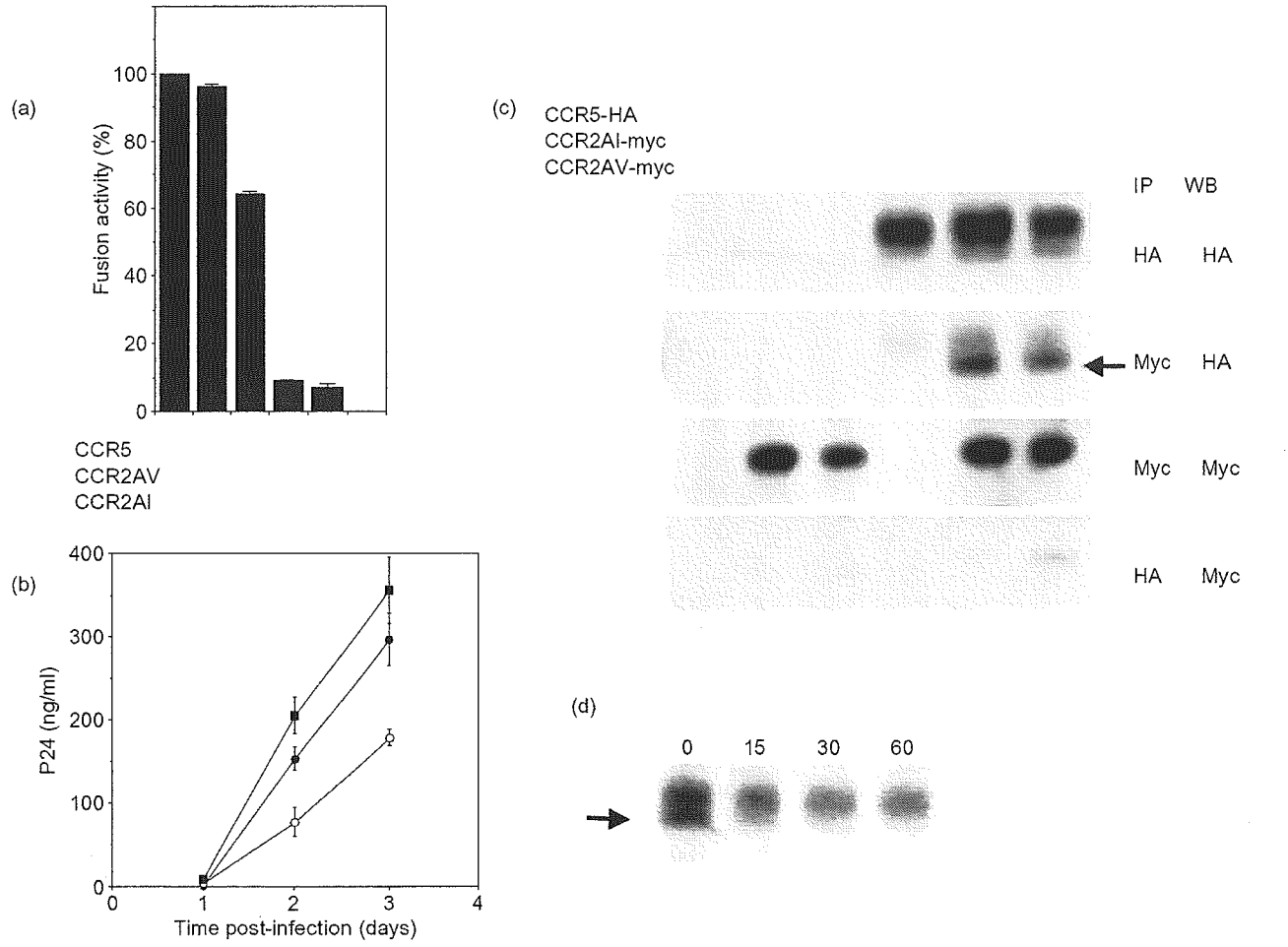

Fig. 5. (a) Coreceptor activity of CCR5 in CCR2A-64V or CCR2A-64I co-expressed cells. SeV vector was used to express CCR2A-64V or CCR2A-64I, and Vac vector was used to express CCR5 as described in Fig. 4. HIV-1 coreceptor activity of each sample was measured using the method described in Materials and methods. The wild-type Vac WR strain was used as a CCR5-negative control, and the wild-type SeV Z strain was used as the CCR2A-negative control. (b) MT4 cells were co-infected with SeV expressing CCR5 and SeV expressing CCR2A-64V (filled circles), CCR2A-64I (open circles), or parental Z strain (filled squares). Five hours after infection, cells were inoculated with an HIV-1 strain SF162. (c) Co-immunopresipitation of CCR2A and CCR5. Recombinant Vac expressing CCR5-HA or parental WR strain (–) was superinfected in CV1 cells infected with SeVs expressing CCR2A-64V-myc, CCR2A-64I-myc, or the parental Z strain (–). Immunoprecipitation and Western blot analysis were performed by using anti-HA or anti-myc antibody. An arrow indicates 37-kDa CCR5-HA molecules. (d) Pulse-chase analysis of CCR5 molecules. A recombinant Vac expressing CCR5-HA was inoculated into CV1 cells. An arrow indicates 37-kDa CCR5-HA molecules.

interferes with the maturation process of CCR5 molecules in cytoplasm.

Discussion

Many independent cohort studies have affirmed the AIDS-delaying effects of the *CCR2-64I* allele [4–8], but the molecular mechanism of this protective effect had not yet been elucidated. In the present study, we demonstrated that a valine to isoleucine substitution at position 64 increased stability of CCR2A but not of CCR2B molecules in cells. When co-expressed with the major HIV-1 co-receptor CCR5, CCR2A-64I more severely interfered with cell surface expression as well as HIV-1 co-receptor activity of CCR5 than CCR2A-64V. Furthermore, CCR2A was shown to co-precipitate with immature form of CCR5. These results suggest that CCR2A binds to CCR5 in the cytoplasm and dominantly interferes with CCR5 maturation and surface expression. On the other hand, the 64I substitution did not affect the level of CCR2B expression, being consistent with results published previously [9,10]. We speculate that increased ability of CCR2A-64I to down modulate CCR5 expression

might be a possible cause of delay in HIV-1 disease progression in patients with this allele. Alternatively, it is also possible that immune cell trafficking and/or signalling might be affected by CCR2A stabilization, leading to a delay in HIV-1 diseases.

Previously, Mellado *et al.* reported that CXCR4 could dimerize with CCR2B-64I variants but not with wild-type CCR2B-64V upon stimulation with SDF-1 and MCP-1. Based on this finding, they proposed that this ability of CCR2B-64I to heterodimerize with CXCR4 may cause a delay in AIDS progression [20]. However, several independent cohort studies have shown that the effects of the *CCR2-64I* allele were more pronounced in earlier stages of disease than in latter stages [5,8,21]. In a Dutch cohort, delay in HIV-1 disease progression was more pronounced before the emergence of X4 variants and was not observed after the emergence of X4 variants in individuals with the CCR2-64I allele [6]. Therefore, it is unlikely that CCR2B-64I/CXCR4 heterodimerization is the main cause of delay in AIDS progression in individuals with CCR2-64I.

Previous studies exploring the oligomerization of chemokine receptors also yielded controversial results. Rodrigues-Frade *et al.* reported that CCR2B forms homodimers upon stimulation by MCP-1 [22]. Other studies, however, have shown that CCR5 [23,24] and CXCR4 [25] can form homodimers without any stimulation by their ligands. Although we did not test whether or not stimulation with MCP-1 and/or RANTES increases hetero-oligomer formation between CCR2A and CCR5, our present results support the latter model that chemokine receptors may form oligomers without stimulation by their ligands.

In addition to AIDS pathogenesis, the CCR2-64I allele was reported to be associated with lower risks of coronary artery calcification [26] and acute rejection in renal transplantation [27]. Our present results shed light onto possible mechanisms of the association of this allele with such diverse human phenotypes. It is now widely accepted that monocyte attachment to cardiovascular wall is the first event implicated in atherogenesis of coronary arteries [28,29]. Since monocytes are known to express both CCR2A and CCR2B [13], an increased stability of CCR2A resulting from the 64I substitution may interfere with the function of CCR2B in monocytes, leading to decreased monocyte invasion to cardiovascular walls. With respect to acute rejection in renal transplantation, CCR5 is known to play an important role in both rejection of renal transplantation [30] and experimental graft-versus-host disease models [31]. Therefore, it is possible that an increased ability of CCR2A-64I to interfere with CCR5 expression can cause a decreased frequency of acute rejection after renal transplantation in recipients with this allele.

Previous studies have failed to show a statistically significant difference in levels of CCR5 expression on stimulated or non-stimulated peripheral blood mononuclear cells between CCR2-64I homozygotes and CCR2-64V homozygotes [9,10,32], although a slight reduction was noted in CCR2-64I homozygotes. In fact, we also failed to observe a statistically significant reduction of CCR5 levels on peripheral CD4 cells of homozygotes of CCR2-64I (data not shown). CCR2 is reported to be expressed on monocytes/macrophages [33], basophils [34,35], B cells [36], NK cells [37], dendritic cells [38,39], and a limited population of T cells [40]. Although we observed very few CCR2 cells in peripheral blood mononuclear cells, Bartoli *et al.* reported that numerous mononuclear cells in tonsil expressed CCR2A [41]. It may be possible that specific cell types expressing both CCR2A and CCR5 in tonsil or lymph nodes play an important role in AIDS pathogenesis and are responsible for the delay in HIV-1 diseases observed in patients with CCR2-64I.

Acknowledgements

pGIT7 beta-gal was kindly supplied by E. Berger. We thank D. Chao for critical discussion and S. Bando for technical assistance.

Sponsorship: Supported by grants from the Human Science Foundation, the Ministry of Education, Culture, Sports, Science, and Technology, and the Ministry of Health, Labour and Welfare, Japan.

References

1. Doranz BJ, Rucker J, Yi Y, Smyth RJ, Samson M, Peiper SC, *et al.* **A dual-tropic primary HIV-1 isolate that uses fusin and the beta-chemokine receptors CKR-5, CKR-3, and CKR-2b as fusion cofactors.** *Cell* 1996, 85:1149–1158.
2. Rucker J, Edinger AL, Sharron M, Samson M, Lee B, Berson JF, *et al.* **Utilization of chemokine receptors, orphan receptors, and herpesvirus- encoded receptors by diverse human and simian immunodeficiency viruses.** *J Virol* 1997, 71:8999–9007.
3. Penton-Rol G, Cota M, Polentarutti N, Luini W, Bernasconi S, Borsatti A, *et al.* **Up-regulation of CCR2 chemokine receptor expression and increased susceptibility to the multitropic HIV strain 89.6 in monocytes exposed to glucocorticoid hormones.** *J Immunol* 1999, 163:3524–3529.
4. Smith MW, Dean M, Carrington M, Winkler C, Huttley GA, Lomb DA, *et al.* **Contrasting genetic influence of CCR2 and CCR5 variants on HIV-1 infection and disease progression. Hemophilia Growth and Development Study (HGDS), Multicenter AIDS Cohort Study (MACS), Multicenter Hemophilia Cohort Study (MHCS), San Francisco City Cohort (SFCC), ALIVE Study.** *Science* 1997, 277:959–965.
5. Kostrikis LG, Huang Y, Moore JP, Wolinsky SM, Zhang L, Guo Y, *et al.* **A chemokine receptor CCR2 allele delays HIV-1 disease progression and is associated with a CCR5 promoter mutation.** *Nat Med* 1998, 4:350–353.
6. van Rij RP, de Roda Husman AM, Brouwer M, Goudsmit J, Coutinho RA, Schuitemaker H. **Role of CCR2 genotype in the clinical course of syncytium-inducing (SI) or non-SI human immunodeficiency virus type 1 infection and in the time to**

conversion to SI virus variants. *J Infect Dis* 1998, **178**: 1806–1811.

7. Ioannidis JP, Rosenberg PS, Goedert JJ, Ashton LJ, Benfield TL, Buchbinder SP, *et al.* **Effects of CCR5-Delta32, CCR2-641, and SDF-1 3'A alleles on HIV-1 disease progression: An international meta-analysis of individual- patient data.** *Ann Intern Med* 2001, **135**:782–795.
8. Mulherin SA, O'Brien TR, Ioannidis JP, Goedert JJ, Buchbinder SP, Coutinho RA, *et al.* **Effects of CCR5-Delta32 and CCR2-641 alleles on HIV-1 disease progression: the protection varies with duration of infection.** *AIDS* 2003, **17**:377–387.
9. Lee B, Doranz BJ, Rana S, Yi Y, Mellado M, Frade JM, *et al.* **Influence of the CCR2-V641 polymorphism on human immunodeficiency virus type 1 coreceptor activity and on chemokine receptor function of CCR2b, CCR3, CCR5, and CXCR4.** *J Virol* 1998, **72**:7450–7458.
10. Mariani R, Wong S, Mulder LC, Wilkinson DA, Reinhart AL, LaRosa G, *et al.* **CCR2-641 polymorphism is not associated with altered CCR5 expression or coreceptor function.** *J Virol* 1999, **73**:2450–2459.
11. Mummidi S, Ahuja SS, Gonzalez E, Anderson SA, Santiago EN, Stephan KT, *et al.* **Genealogy of the CCR5 locus and chemokine system gene variants associated with altered rates of HIV-1 disease progression.** *Nat Med* 1998, **4**: 786–793.
12. Charo IF, Myers SJ, Herman A, Franci C, Connolly AJ, Coughlin SR. **Molecular cloning and functional expression of two monocyte chemoattractant protein 1 receptors reveals alternative splicing of the carboxyl-terminal tails.** *Proc Natl Acad Sci USA* 1994, **91**:2752–2756.
13. Wong LM, Myers SJ, Tsou CL, Gosling J, Arai H, Charo IF. **Organization and differential expression of the human monocyte chemoattractant protein 1 receptor gene. Evidence for the role of the carboxyl-terminal tail in receptor trafficking.** *J Biol Chem* 1997, **272**:1038–1045.
14. Sanders SK, Crean SM, Boxer PA, Kellner D, LaRosa GJ, Hunt SW, 3rd. **Functional differences between monocyte chemotactic protein-1 receptor A and monocyte chemotactic protein-1 receptor B expressed in a Jurkat T cell.** *J Immunol* 2000, **165**:4877–4883.
15. Louisirirotchanakul S, Liu H, Roongpisuthipong A, Nakayama EE, Takebe Y, Shioda T, *et al.* **Genetic analysis of HIV-1 discordant couples in Thailand: association of CCR2 641 homozygosity with HIV-1-negative status.** *J Acquir Immune Defic Syndr* 2002, **29**:314–315.
16. Kato A, Sakai Y, Shioda T, Kondo T, Nakanishi M, Nagai Y. **Initiation of Sendai virus multiplication from transfected cDNA or RNA with negative or positive sense.** *Genes Cells* 1996, **1**:569–579.
17. Shioda T, Nakayama EE, Tanaka Y, Xin X, Liu H, Kawana-Tachikawa A, *et al.* **Naturally occurring deletional mutation in the C-terminal cytoplasmic tail of CCR5 affects surface trafficking of CCR5.** *J Virol* 2001, **75**:3462–3468.
18. Shioda T, Kato H, Ohnishi Y, Tashiro K, Ikegawa M, Nakayama EE, *et al.* **Anti-HIV-1 and chemotactic activities of human stromal cell-derived factor 1alpha (SDF-1alpha) and SDF-1beta are abolished by CD26/dipeptidyl peptidase IV-mediated cleavage.** *Proc Natl Acad Sci USA* 1998, **95**:6331–6336.
19. Nakayama EE, Shioda T, Tatsumi M, Xin X, Yu D, Ohgimoto S, *et al.* **Importance of the N-glycan in the V3 loop of HIV-1 envelope protein for CXCR-4- but not CCR-5-dependent fusion.** *FEBS Lett* 1998, **426**:367–372.
20. Mellado M, Rodriguez-Frade JM, Vila-Coro AJ, de Ana AM, Martinez AC. **Chemokine control of HIV-1 infection.** *Nature* 1999, **400**:723–724.
21. Michael NL, Louie LG, Rohrbaugh AL, Schultz KA, Dayhoff DE, Wang CE, *et al.* **The role of CCR5 and CCR2 polymorphisms in HIV-1 transmission and disease progression.** *Nat Med* 1997, **3**:1160–1162.
22. Rodriguez-Frade JM, Vila-Coro AJ, de Ana AM, Albar JP, Martinez AC, Mellado M. **The chemokine monocyte chemoattractant protein-1 induces functional responses through dimerization of its receptor CCR2.** *Proc Natl Acad Sci USA* 1999, **96**: 3628–3633.
23. Benkirane M, Jin DY, Chun RF, Koup RA, Jeang KT. **Mechanism of transdominant inhibition of CCR5-mediated HIV-1 infection by ccr5delta32.** *J Biol Chem* 1997, **272**:30603–30606.
24. Issafras H, Angers S, Bulenger S, Blanpain C, Parmentier M, Labbe-Jullie C, *et al.* **Constitutive agonist-independent CCR5 oligomerization and antibody- mediated clustering occurring at physiological levels of receptors.** *J Biol Chem* 2002, **277**: 34666–34673.
25. Babcock GJ, Farzan M, Sodroski J. **Ligand-independent dimerization of CXCR4, a principal HIV-1 coreceptor.** *J Biol Chem* 2003, **278**:3378–3385.
26. Valdes AM, Wolfe ML, O'Brien EJ, Spurr NK, Gefter W, Rut. A, *et al.* **Val641le polymorphism in the C-C chemokine receptor 2 is associated with reduced coronary artery calcification.** *Arterioscler Thromb Vasc Biol* 2002, **22**:1924–1928.
27. Abdi R, Tran TB, Sahagun-Ruiz A, Murphy PM, Brenner BM, Milford EL, *et al.* **Chemokine receptor polymorphism and risk of acute rejection in human renal transplantation.** *J Am Soc Nephrol* 2002, **13**:754–758.
28. Ross R. **The pathogenesis of atherosclerosis: a perspective for the 1990s.** *Nature* 1993, **362**:801–809.
29. Hanke H, Lenz C, Finking G. **The discovery of the pathophysiological aspects of atherosclerosis–a review.** *Acta Chir Belg* 2001, **101**:162–169.
30. Segerer S, Cui Y, Eitner F, Goodpaster T, Hudkins KL, Mack M, *et al.* **Expression of chemokines and chemokine receptors during human renal transplant rejection.** *Am J Kidney Dis* 2001, **37**:518–531.
31. Murai M, Yoneyama H, Harada A, Yi Z, Vestergaard C, Guo B, *et al.* **Active participation of CCR5(+)CD8(+) T lymphocytes in the pathogenesis of liver injury in graft-versus-host disease.** *J Clin Invest* 1999,104:49-57.
32. Shieh B, Liau YE, Hsieh PS, Yan YP, Wang ST, Li C. **Influence of nucleotide polymorphisms in the CCR2 gene and the CCR5 promoter on the expression of cell surface CCR5 and CXCR4.** *Int Immunol* 2000, **12**:1311–1318.
33. Fantuzzi L, Borghi P, Ciolli V, Pavlakis G, Belardelli F, Gessani S. **Loss of CCR2 expression and functional response to monocyte chemotactic protein (MCP-1) during the differentiation of human monocytes: role of secreted MCP-1 in the regulation of the chemotactic response.** *Blood* 1999, **94**:875–883.
34. Ochensberger B, Tassera L, Bifrare D, Rihs S, Dahinden CA. **Regulation of cytokine expression and leukotriene formation in human basophils by growth factors, chemokines and chemotactic agonists.** Eur *J Immunol* 1999, **29**:11–22.
35. Iikura M, Miyamasu M, Yamaguchi M, Kawasaki H, Matsushima K, Kitaura M, *et al.* **Chemokine receptors in human basophils: inducible expression of functional CXCR4.** *J Leukoc Biol* 2001, **70**:113–120.
36. Frade JM, Mellado M, del Real G, Gutierrez-Ramos JC, Lind P, Martinez AC. **Characterization of the CCR2 chemokine receptor: functional CCR2 receptor expression in B cells.** *J Immunol* 1997, **159**:5576–5584.
37. Polentarutti N, Allavena P, Bianchi G, Giardina G, Basile A, Sozzani S, *et al.* **IL-2-regulated expression of the monocyte chemotactic protein-1 receptor (CCR2) in human NK cells: characterization of a predominant 3.4-kilobase transcript containing CCR2B and CCR2A sequences.** *J Immunol* 1997, **158**:2689–2694.
38. Sallusto F, Schaerli P, Loetscher P, Schaniel C, Lenig D, Mackay CR, *et al.* **Rapid and coordinated switch in chemokine receptor expression during dendritic cell maturation.** Eur *J Immunol* 1998, **28**:2760–2769.
39. Vanbervliet B, Homey B, Durand I, Massacrier C, Ait-Yahia S, de Bouteiller O, *et al.* **Sequential involvement of CCR2 and CCR6 ligands for immature dendritic cell recruitment: possible role at inflamed epithelial surfaces.** Eur *J Immunol* 2002, **32**:231–242.
40. Rabin RL, Park MK, Liao F, Swofford R, Stephany D, Farber JM. **Chemokine receptor responses on T cells are achieved through regulation of both receptor expression and signaling.** *J Immunol* 1999, **162**:3840–3850.
41. Bartoli C, Civatte M, Pellissier JF, Figarella-Branger D. **CCR2A and CCR2B, the two isoforms of the monocyte chemoattractant protein-1 receptor are up-regulated and expressed by different cell subsets in idiopathic inflammatory myopathies.** *Acta Neuropathol (Berl)* 2001, **102**:385–392.

Cross-Talk between Activated Human NK Cells and CD4 T Cells via OX40-OX40 Ligand Interactions[1]

Alessandra Zingoni,*† Thierry Sornasse,[2‡] Benjamin G. Cocks,‡ Yuetsu Tanaka,§ Angela Santoni,† and Lewis L. Lanier[3]*

It is important to understand which molecules are relevant for linking innate and adaptive immune cells. In this study, we show that OX40 ligand is selectively induced on IL-2, IL-12, or IL-15-activated human NK cells following stimulation through NKG2D, the low affinity receptor for IgG (CD16) or killer cell Ig-like receptor 2DS2. CD16-activated NK cells costimulate TCR-induced proliferation, and IFN- produced by autologous CD4 T cells and this process is dependent upon expression of OX40 ligand and B7 by the activated NK cells. These findings suggest a novel and unexpected link between the natural and specific immune responses, providing direct evidence for cross-talk between human CD4 T cells and NK receptor-activated NK cells. *The Journal of Immunology,* **2004, 173: 3716–3724.**

For an effective T cell response at least two signals are needed: the first is delivered by TCR interaction with MHC and peptide, and the second involves ligation of costimulatory receptors. Costimulation can involve augmenting cell proliferation, cell survival, and/or the production of cytokines. Many receptors have now been described to be costimulatory, including receptors of the Ig superfamily, such as CD28 and ICOS, and receptors of the TNF superfamily. Interactions between TNF ligands and TNFR family members, including for example OX40 ligand (OX40L) and OX40, have been implicated in T cell costimulation (1). Expression of OX40L is inducible and has been reported on several hemopoietic cell types, including dendritic cells (2), B cells (3), T cells, and microglial cells, as well as on vascular endothelial cells (4). OX40L expression is induced on APCs several days after activation by CD40L-CD40 interactions or by inflammatory stimuli (1, 2). Recently, high levels of OX40L have been shown to be expressed on a new type of CD3 CD4 accessory cell, located in B cell follicles, capable of promoting survival of Th2 cells through OX40-OX40L interactions (5). OX40 is expressed predominantly by activated CD4 T cells (6). OX40 cells are found in the T cell zones of lymphoid organs following priming with Ag (3), and also have been detected in situ in several inflammatory states, including experimental autoimmune encephalomyelitis, rheumatoid arthritis, chronic synovitis, graft-vs-host disease, and on tumor-infiltrating lymphocytes (6–9). Ligation of OX40 on CD4 T cells by agonist reagents can increase clonal expansion and cytokine production (10), enhance memory T cell development (11), and augment anti-tumor immunity (12). OX40 has also been shown to play an important role in the stimulation of anti-viral CD4 T cell responses in vivo (13).

NK cells are lymphocytes that provide innate immunity against tumors and virus-infected cells. A balance of signals received from multiple activating and inhibitory receptors regulates their effector functions (14). These receptors allow NK cells to rapidly survey their environment for danger. When an imbalance in signaling favors activation, secretion of cytokines and/or release of cytotoxic granules occurs (14). In humans, NKG2D is one of the activating receptors that is expressed on NK cells, T cells, and CD8 T cells (15). NKG2D recognizes as ligands UL16-binding protein 1 (ULBP1), ULBP2, ULBP3, ULBP4, and the MHC class I chain-related molecules, MICA and MICB (15, 16). These NKG2D ligands are generally absent or expressed at low levels on most healthy cells, but can be induced by viral (17) and bacterial infections (18, 19). In addition, they are frequently up-regulated in many epithelial tumors (20) and in "stressed" cells (21).

Several studies have focused on the ability of NK cells to regulate adaptive immune responses through the production of Th1-type cytokines early during infection (22) or through the activation of dendritic cells (23). In addition, by establishing cocultures of NK- and Ag-activated T cells, it has been shown that human NK cells can be induced to secrete IFN- in response to IL-2 produced by activated T cells (24). In contrast, much less has been reported about the physical interactions that may take place between NK cells and adaptive immune cells, in particular CD4 T cells.

In this study, we show that OX40L can be induced on human NK cells by stimulation through their activating NK receptors. In addition, we present direct evidence for cross-talk between CD4 T cells and NK cells in which OX40-OX40L and CD28-B7 interactions contribute to T cell proliferation and IFN- production in response to TCR-induced activation.

Materials and Methods

Reagents, cytokines, Abs, and flow cytometry

Human rIL-12 and IL-15 were purchased from BioSource International (Camarillo, CA). The National Cancer Institute Biological Resources

*Department of Microbiology and Immunology and the Cancer Research Institute, University of California, San Francisco, CA 94143; †Department of Experimental Medicine and Pathology, University of Rome "La Sapienza", Rome, Italy; ‡Incyte Corporation, Palo Alto, CA 94304; and §Department of Immunology, Graduate School and Faculty of Medicine, University of the Ryukyus, Okinawa, Japan

Received for publication May 18, 2004. Accepted for publication June 18, 2004.

The costs of publication of this article were defrayed in part by the payment of page charges. This article must therefore be hereby marked *advertisement* in accordance with 18 U.S.C. Section 1734 solely to indicate this fact.

[1] L.L.L. is an American Cancer Society Research Professor, and A.Z. was a recipient of an American-Italian Cancer Foundation Fellowship and of a research contract with the University of Rome "La Sapienza". These studies were supported by National Institutes of Health Grant CA89294 and a grant from Associazione Italiana per la Ricerca sul Cancro to A.S.

[2] Current address: Protein Design Labs, Inc., Pre-Clinical and Clinical Development Sciences, 34801 Campus Drive, Fremont, CA 94555.

[3] Address correspondence and reprint requests to Dr. Lewis L. Lanier, Department of Microbiology and Immunology and the Cancer Research Institute, University of California, 513 Parnassus Avenue, San Francisco, CA 94143. E-mail address: lanier@itsa.ucsf.edu

[4] Abbreviations used in this paper: OX40L, OX40 ligand; cIg, control Ig; SEB, staphylococcal enterotoxin B; ULBP, UL16-binding protein; KIR, killer cell Ig-like receptor.

0022-1767/04/$02.00

Branch Preclinical Repository (Frederick, MD) generously provided human rIL-2. Staphylococcal enterotoxin B (SEB) and PHA were purchased from Sigma-Aldrich (St. Louis, MO). The following mouse anti-human mAbs were used: anti-killer cell Ig-like receptor (KIR)2DS2 (DX27), neutralizing anti-CD80 (L307), and anti-CD86 (IT2.2) (BD Pharmingen, San Diego, CA), FITC-conjugated anti-CD80 (BU63; Caltag Laboratories, Burlingame, CA), FITC-conjugated anti-CD86 (MEM-233; Caltag Laboratories), anti-CD8 (Leu2a; BD Pharmingen), anti-CD4 (Leu3a; BD Pharmingen), anti-HLA-DR (BD Pharmingen), anti-NKG2D (clone 149810; R&D Systems, Minneapolis, MN), anti-CD56 (DX32), neutralizing anti-OX40L (5A8) (2, 4), anti-CD16 (B73.1) (kindly provided by Dr. G. Trinchieri, Schering-Plough, Dardilly, France), and anti-CD3 (OKT3; American Tissue Culture Collection, Manassas, VA). PE-conjugated goat anti-mouse IgG was purchased from Jackson ImmunoResearch Laboratories (West Grove, PA), FITC-conjugated anti-mouse IgG was purchased from Zymed Laboratories (South San Francisco, CA), and goat anti-mouse IgG F(ab)$_2$ was from Cappel Laboratories (ICN Biomedicals, Opera, Milan, Italy). Cells were analyzed by using a FACSCalibur (BD Biosciences, San Jose, CA) or a small desktop Guava Personal Cytometer with Guava ViaCount and Guava Express software (Burlingame, CA). Viable lymphocyte populations were gated based on forward and side scatters and by propidium iodide staining.

Cell lines, plasmids, and transfectants

The NKL cell line, generously provided by Dr. Mike Robertson (25), was cultured in RPMI 1640 medium supplemented with 10% FCS, 2 mM L-glutamine, 100 U/ml penicillin, 100 g/ml streptomycin, and 200 U/ml human rIL-2. Cells were cultured at a density of 5 10^5/ml in a 37°C incubator with 5% CO_2. For all experiments, cells were grown at a density of 1 10^6/ml in medium containing IL-2. Generation of NKL stably expressing KIR2DS2 was described previously (26). Because mouse Ba/F3 pro-B cells are IL-3 dependent for their proliferation, the Ba/F3 cells used in these experiments were transfected with an expression plasmid containing the mouse cDNA IL-3 to provide for autocrine growth (kindly provided by Dr. S. Tangye, Centenary Institute, Sydney, Australia). MICA transfectants were established by retroviral transduction using the pMX-pie vector (27, 28) containing a MICA*0019 cDNA.

Preparation of NK cells and T cells

Small resting CD4 T lymphocytes were purified as follows: PBMC were isolated by lymphoprep density gradient centrifugation, monocytes and B cells were removed by adherence to nylon wool, then cells were labeled with anti-CD8, anti-CD56, anti-HLA-DR, and anti-CD19 mAbs, and these cells were mixed with magnetic beads coated with goat anti-mouse IgG (Dynal Biotech, Oslo, Norway). Thereafter, CD8 , CD19 , HLA-DR , and CD56 cells were removed by magnetic cell sorting. The remaining cells were 98% CD4 CD3 , as assessed by immunofluorescence and flow cytometric analysis. Polyclonal NK cell cultures were obtained by coculturing nylon nonadherent PBMC with irradiated (3000 rad) RPMI 8866 B cells for 9–10 days at 37°C in a humidified 5% CO_2 atmosphere, as previously described (29). NK cell cultures were 90% CD16 CD56 CD3 , as assessed by immunofluorescence and flow cytometric analysis. Contaminating T cells were depleted by magnetic cell sorting, yielding a final NK population 98% CD16 CD56 CD3 .

Stimulation of the cells, RNA preparation, microarrays, and data analysis

Twenty-four-well culture plates were coated with goat anti-mouse IgG (5 g/ml, in carbonate buffer, pH 9.6) at 37°C for 4 h. Wells were washed three times with PBS and primary Abs were added to each well at 10 g/ml, or amounts indicated in the figures, and incubated overnight at 4°C in PBS. When in combination with anti-NKG2D mAb, anti-KIR2DS2 mAb was used at 0.5 g/ml. NKL cells were plated at 2 10^6/ml in each well in 500 l of medium. Poly(A) RNA was isolated using an mRNA isolation kit (Qiagen, Valencia, CA) according to the manufacturer's protocol. Gene expression modulation between unstimulated and stimulated NKL cells was evaluated by using Incyte standard procedures (Palo Alto, CA), as described elsewhere (30). Briefly, poly(A) RNA were labeled with Cy3 or Cy5 fluorescent labeling dyes using reverse transcription, followed by hybridization onto a Human Drug Target 1 microarray (Incyte) (31, 32). This microarray contained a total of 9129 elements representing a total of 8481 unique gene clusters whose identity was confirmed by stringent PCR verification during manufacturing. The Cy3/Cy5 ratio for each element was considered valid if the signal to background ratios for both dyes exceeded 2.5, and if the signal of either dye exceeded 250 fluorescence units. A total of 6125 elements returned valid Cy3/Cy5 ratios for all 20 hybridizations (10 treatments hybridized in duplicates). Elements were further selected based on a minimum Cy3/Cy5 ratio of 2-fold in either direction in at least one experimental condition, yielding 406 elements of interest. These elements of interest were then clustered using an agglomerative clustering algorithm (Ward's method, JMP; SAS Institute, Cary, NC). All data are expressed in $\log_2$, where negative values denote gene up-regulation (Cy3 Cy5) and reciprocally, positive values represent gene down-regulation (Cy3 Cy5).

Cytokine and proliferation assays

Homogeneous populations of cultured human primary NK cells were activated for 72 h with IL-2 (100 U/ml) and stimulated with anti-CD16 plate-bound mAb for 18 h. In some experiments, NK cells were preactivated with IL-15 (10 ng/ml) or IL-12 (10 U/ml). Dead cells were removed by Ficoll-gradient centrifugation. NK cells were fixed with 1% paraformaldehyde (in PBS, pH 7.4) for 7 min at room temperature. Different numbers of NK cells were plated with 1 10^5 highly purified autologous CD4 T cells, and cultured for 5 days in the presence of soluble anti-CD3 mAb (5 g/ml) or SEB (0.5–25 ng/ml) or PHA (50 ng/ml). Blocking Ab against OX40L and/or CD80 and CD86 was added on day 0 at 5 g/ml. Wells were pulsed with 0.5 Ci of [^{3}H]thymidine for the final 18 h of culture, and incorporated radioactivity was measured in a scintillation counter. Data are represented as the mean of cpm SD (triplicates). In some experiments, supernatants were collected at day 3 or 5, and the amount of IL-4 and IFN- was quantified by specific ELISA kits (BioSource International).

Results

Microarray analysis shows up-regulation of OX40L following triggering of NK-activating receptors on a human NK cell line

Microarray analysis was used to characterize genes up-regulated by the stimulation of NKG2D alone or in combination with the DAP12-associated KIR2DS2-activating receptor. As a model, we used a human NK cell line, NKL, which constitutively expresses the DAP10-associated NKG2D receptor (33), and was transfected with KIR2DS2 (26). Because NKG2D alone is an insufficient stimulus for the transcription-dependent production of IFN- (26, 34), this cell system is particularly useful because it provided the opportunity to evaluate the efficacy of NKG2D costimulation using as a read out the amplification of KIR2DS2-induced IFN- (Ref. 26 and data not shown). Poly(A) mRNA from resting and stimulated NKL cells was extracted, and cDNA was prepared for the comprehensive analysis of gene transcription by using microarray technology. A Human Drug Target 1 Incyte microarray containing a total of 9128 elements was used. Analysis of data was performed using a hierarchical clustering algorithm to group genes with similar expression patterns across all the samples. We focused our attention on a group of seven genes that were amplified significantly following the simultaneous cross-linking of KIR2DS2 and NKG2D receptors (Table I). These genes included three chemokines (i.e., lymphotactin, MIP-1 , and CCL18), granzymes B and H, the platelet-activating receptor homologue (a seven transmembrane receptor of unknown function), and the TNF member OX40L (CD134L). Among this group of genes, OX40L mRNA was the only one that was up-regulated by NKG2D cross-linking alone (Table I). Previously, OX40L expression has been implicated predominantly in the function of APCs, such as activated monocytes, dendritic cells, and B cells. Thus, this unexpected finding prompted us to investigate the role of OX40L in human NK cell function.

Results from the microarray experiment were confirmed by showing that cross-linking KIR2DS2, NKG2D, and KIR2DS2 plus NKG2D indeed enhanced transcription of OX40L in NKL cells, as determined by quantitative RT-PCR analysis (data not shown). More importantly, KIR2DS2- and NKG2D-induced activation resulted in an increased expression of OX40L on the cell surface of NKL cells, as determined by using a specific anti-OX40L mAb

Table 1. *Microarray analysis of NKL cells stimulated through NKG2D and/or KIR2DS2*[a]

Gene Name	Accession Number	cIg	KIR2DS2	NKG2D	KIR2DS2 NKG2D
Lymphotactin	AL031736	0.31	0.85	0.48	2.39
MIP-1	AV758471	0.06	1.03	0.07	2.14
Granzyme H	NM_004131	0.43	0.58	0.96	1.87
Granzyme B	M57888	0.12	0.48	0.81	1.74
PAR	NM_013308	0.32	0.72	0.07	1.63
OX40L	**BE349175**	**0.13**	**0.68**	**0.20**	**1.26**
CCL18	NM_00298	0.48	0.58	0.14	1.42

[a] Differential expression ratios of control Ig (cIg)-treated NKL cells (Cy3) compared to anti-KIR2DS2 and/or anti-NKG2D-treated NKL cells (Cy5) expressed in $\log_2$. Negative values represent up-regulation of transcription compared with cIg-stimulated cells.

(Fig. 1*A*). Stimulation with high doses of anti-KIR mAb or anti-NKG2D mAb alone substantially up-regulated OX40L on the surface of NKL cells. In addition, anti-NKG2D mAb augmented up-regulation of OX40L on NKL cells stimulated with a suboptimal dose of anti-KIR mAb (Fig. 1*A*).

OX40 is expressed predominantly on activated CD4 T cells and prior studies have shown that interactions between OX40 on activated CD4 T cells and OX40L on APCs can augment T cell proliferation and cytokine production. Therefore, studies were performed to determine whether OX40L-bearing NK cells could costimulate CD4 T cell proliferation. NKL cells, which constitutively express OX40L (Fig. 1*A*), were cocultured with freshly isolated human CD4 T cells and were stimulated with anti-CD3 mAb or PHA. As shown in Fig. 1*B*, NKL indeed augmented CD4 T cell proliferation, and this activity was blocked, in part, in the presence of a neutralizing anti-OX40L mAb. These studies indicated that OX40L on NKL is functional and contributes to the proliferation of CD4 T cells. However, these studies were complicated by the necessity to use allogeneic CD4 T cells and also because NKL is a long-term NK cell line established from a patient with NK cell leukemia (25). Therefore, it was important to validate these findings using autologous NK cells and T cells from normal healthy individuals.

Both cytokines and NK receptor-mediated stimulation are required to induce OX40L on human peripheral blood NK cells

Freshly isolated, highly purified human peripheral blood NK cells do not express OX40L on the cell surface (data not shown), although a prior study had reported the presence of OX40L transcripts (35). Because the NKL cell line requires IL-2 for growth, we investigated whether OX40L could be induced on peripheral blood NK cells from healthy adults simply by culture in the presence of IL-2 or other cytokines known to stimulate NK cells, e.g., IL-12 and IL-15. As shown in Fig. 2*A*, culture of normal human peripheral blood NK cells in IL-2, IL-12, or IL-15 failed to induce OX40L. Therefore, based on the observation that OX40L was up-regulated in NKL cells stimulated through its activating receptors, we stimulated human polyclonal NK cells through CD16, an IgG FcR that signals via the ITAM-bearing Fc RI and CD3 adapter proteins. Whereas treatment with cytokines alone failed to induce OX40L, the majority (typically 60% or more) of normal NK cells stimulated by plate-bound anti-CD16 mAb together with IL-2, IL-12, and IL-15 expressed OX40L at high levels on the cell surface (Fig. 2*A*). Stimulation with anti-CD16 mAb in the absence of IL-2 (or IL-12 or IL-15) induced OX40L only on a small proportion of NK cells. A dose-dependent induction of OX40L was observed when NK cells were activated with anti-CD16 mAb in the presence of IL-2 (Fig. 2*B*). In contrast to OX40L, culture of peripheral blood NK cells in IL-2 only did induce expression of CD86 (Fig. 2*C*) and this was not enhanced by stimulation with anti-CD16 mAb (Fig. 2*D*). CD80, another ligand of the CD28 costimulatory receptor on T cells, was not induced by IL-2 (Fig. 2*C*), and there was only a very slight indication of CD80 induction when both IL-2 and anti-CD16 stimulation were combined (Fig. 2*D*).

Because studies using the NKL cell line indicated that stimulation through the NKG2D receptor up-regulated OX40L, we also investigated this using peripheral blood NK cells from healthy adults. Polyclonal populations of NK cells from healthy individuals were expanded in culture, preactivated with IL-2 and stimulated with a plate-bound mAb against NKG2D. Fig. 3*A* shows that NKG2D cross-linking induced OX40L on 20% of the NK cells.

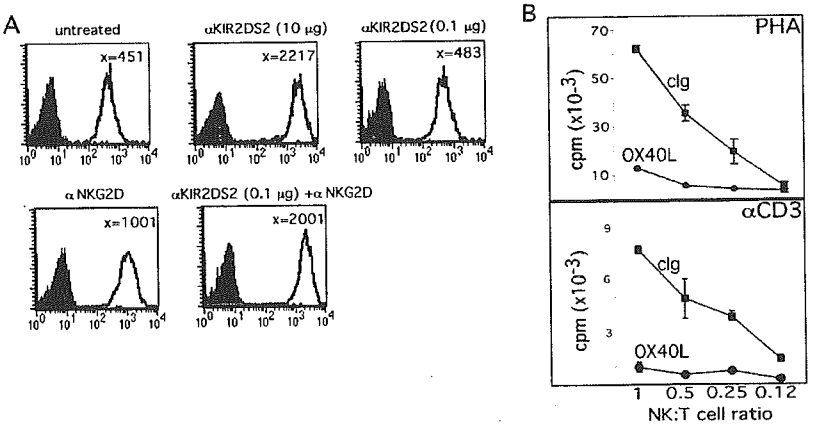

FIGURE 1. Up-regulation of OX40L on NKL by NK receptors and costimulation of CD4 T cell proliferation. *A*, NKL cells were stimulated with plate-bound mAb anti-NKG2D (10 g/ml), anti-KIR2DS2 (10 g/ml or 0.1 g/ml), or both for 18 h. Cells were harvested and stained with PE-conjugated anti-OX40L mAb (open histograms) or with an isotype-matched cIg (filled histograms). *B*, Different amounts of paraformaldehyde-fixed NKL cells were cultured with 1 10^5 CD4 T cells in the presence of soluble anti-CD3 (5 g/ml) or PHA (50 ng/ml). Neutralizing anti-OX40L mAb was added at day 0 and cocultures were harvested at day 5. Cultures were pulsed with 0.5 Ci of [^{3}H]thymidine for the final 18 h, and incorporated radioactivity was measured in a scintillation counter. A representative experiment of three is shown. Data are represented as the mean of cpm SD.

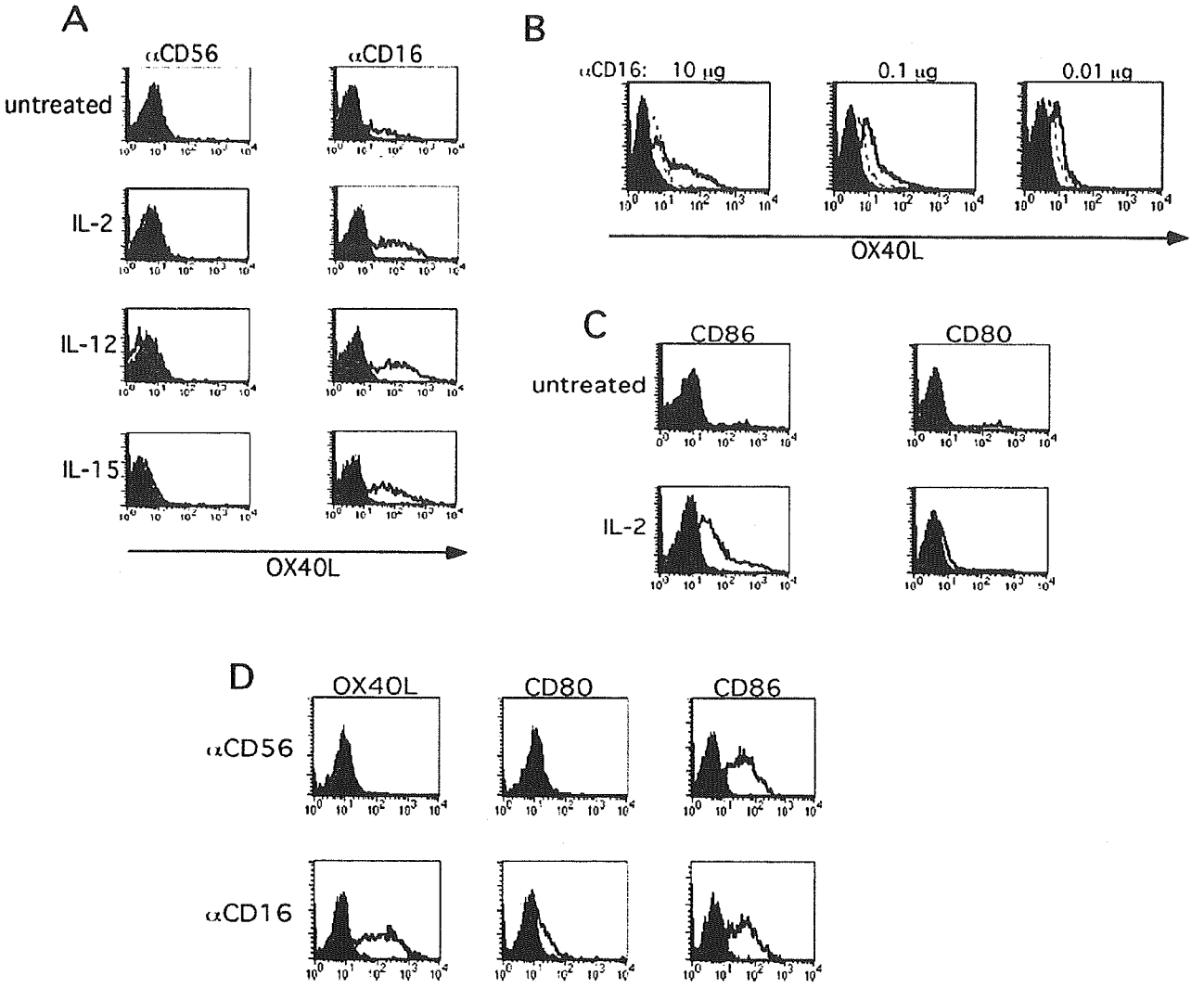

FIGURE 2. Induction of OX40L and B7 family members on human NK cells. *A*, Polyclonal human NK cells were preactivated with IL-2 (200 U/ml), IL-15 (10 ng/ml), or IL-12 (10 U/ml) for 48 h, and stimulated with plate-bound anti-CD16 mAb (saturating concentration). Plate-bound anti-CD56 mAb was used as a negative control. After 18 h of culture, cells were harvested and stained with PE-conjugated anti-OX40L mAb (thick line, open histograms) or with a cIg (filled histograms). *B*, IL-2-activated polyclonal NK cells were stimulated with different amounts (10 g/ml, 0.1 g/ml, and 0.01 g/ml) of plate-bound anti-CD16 mAb (thick line). Plate-bound anti-CD56 mAb (dotted line) was used as a negative control for stimulation. Cells were harvested after 18 h and stained with FITC-conjugated anti-OX40L mAb (open histograms) or a cIg (filled histograms). A representative experiment of five is shown. *C*, Peripheral blood NK cells were cultured in the presence of IL-2 (200 U/ml) for 72 h and stained with FITC–conjugated anti-CD80 (thick lines, open histograms), FITC–conjugated anti-CD86 (thick lines, open histograms), or a cIg (filled histograms). *D*, IL-2-activated polyclonal NK cells were stimulated for 18 h with anti-CD16 or anti-CD56 (negative control) plate-bound mAbs. Cells were stained with PE-conjugated anti-OX40L mAb, FITC–conjugated anti-CD80 (thick lines, open histograms), FITC–conjugated anti-CD86 (thick lines, open histograms), or a cIg (filled histograms). In this experiment, CD86 was induced on these NK cells by coculture in IL-2, but was not further increased by stimulation with the anti-CD56 mAb used as a control.

As observed with anti-CD16 stimulation, induction of OX40L required both pretreatment with IL-2 and NKG2D activation because neither condition alone induced OX40L (data not shown). The ability of NKG2D stimulation to induce OX40L on NK cells was further validated by activation using stimulator cells bearing MICA, a physiological ligand of the NKG2D receptor. IL-2-preactivated peripheral blood NK cells were cocultured for 18 h with different ratios of the mouse pro-B cell line Ba/F3 or Ba/F3 cells stably expressing human MICA. As with anti-NKG2D mAb stimulation, OX40L was induced on 20% of the IL-2-activated NK cells cocultured with MICA Ba/F3 cells, but not the untransfected Ba/F3 cells (Fig. 3*B*). Analysis of the kinetics of OX40L expression on human NK cells following stimulation with MICA-bearing cells showed that OX40L expression was transient; it was expressed rapidly after 5 h, peaked at 18 h, and then declined between 32 to 48 h poststimulation (Fig. 3*C*). These IL-2-activated NK cells were able to efficiently kill the MICA Ba/F3 cells, but not the untransfected Ba/F3 cells, demonstrating that the NKG2D receptor on the NK cells was specifically activated (data not shown).

Therefore, both by stimulation with anti-NKG2D mAb and by interaction with MICA Ba/F3 cells, we observed induction of OX40L on a subset comprising 20% of IL-2-activated peripheral blood NK cells (Fig. 3). An examination of the phenotype of the NK cells stimulated by either anti-NKG2D or MICA Ba/F3 cells revealed that OX40L was induced on both the $CD56^{bright}CD16^{-/low}$ and on the $CD56^{int}CD16^{high}$ peripheral blood NK cell subsets, although within these subsets a relatively higher fraction of the $CD56^{bright}CD16^{-/low}$ NK cells expressed OX40L (our unpublished observation). Therefore, the subset of peripheral blood NK cells presenting OX40L after NKG2D stimulation was not

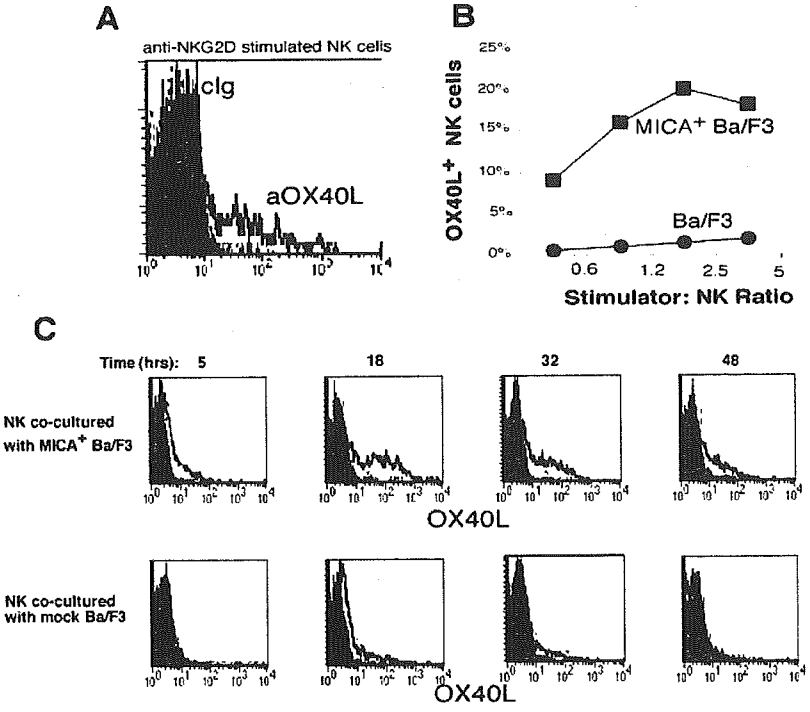

FIGURE 3. NKG2D stimulation induces OX40L on human polyclonal NK cells. *A*, Polyclonal human NK were activated with IL-2 for 72 h and stimulated with plate-bound anti-NKG2D mAb (thick line). Anti-CD56 mAb was used as a negative control of stimulation (dotted line). After 18 h of culture, cells were harvested and stained with FITC-conjugated anti-OX40L mAb (thick line, open histogram) or with cIg (filled histogram). A representative experiment of six is shown. *B*, IL-2-activated polyclonal NK cells were cultured with different numbers of mock Ba/F3 (●) or human MICA Ba/F3 (■) transfectants. After 18 h of coculture, NK cells were stained with anti-OX40L or control mAbs and the percentage of OX40L NK cells is shown. A representative experiment of three is shown. *C*, Kinetics of OX40L induction on NK cells by coculture with NKG2D ligand-bearing cells. IL-2-activated polyclonal NK cells were cultured at a 1:2.5 stimulator:NK cell ratio with mock Ba/F3 (*lower panels*) or MICA Ba/F3 (*upper panels*) transfectants. Cells were harvested after 5, 18, 32, and 48 h of coculture, and stained anti-OX40L mAb (thick line, open histograms) and cIg (filled histograms). A representative experiment of three is shown.

restricted to either of these functionally distinct subsets defined by levels of CD56 and CD16 expression. In experiments combining both anti-NKG2D and anti-CD16 mAb stimulation (using optimal and saturating concentrations of both mAbs), the proportion of peripheral blood NK cells that expressed OX40L was equivalent to using optimal stimulation with anti-CD16 alone (data not shown).

NK cell costimulation of TCR-dependent CD4 T cell proliferation via OX40L-OX40 interactions

Our preliminary studies demonstrated that the OX40L NKL leukemic cells were able to augment the proliferation of allogeneic human resting peripheral blood CD4 T cells stimulated with anti-CD3 mAb or PHA. The proliferation was partially, but substantially, inhibited by using a neutralizing anti-OX40L mAb (Fig. 1*B*). To address the potential interactions between NK cells CD4 T cells in a more physiological context, we performed additional experiments using autologous NK cells and CD4 T cells. We assayed proliferation induced not only by anti-CD3 mAb, but also by using autologous activated human NK cells (that express HLA-DR) to present SEB to autologous resting CD4 T cells. Because we had determined that anti-CD16 was more efficient than anti-NKG2D for inducing OX40L on peripheral blood NK cells, this system was chosen to evaluate the role of OX40L in the interactions between NK cells and autologous CD4 T cells. Highly purified, IL-2-preactivated peripheral blood NK cells were stimulated with anti-CD16 mAb, the NK cells were paraformaldehyde-fixed to prevent their proliferation or secretion of cytokines, and these cells were cocultured at varying ratios with highly purified resting autologous CD4 T cells in the presence of soluble anti-CD3 mAb. As shown in Fig. 4*A*, CD16-activated autologous NK cells efficiently costimulated anti-CD3-induced proliferation of CD4 T cells. This TCR-induced T cell proliferation was in part dependent upon OX40–OX40L interactions, because the proliferation was inhibited on average 60% (based on experiments using NK and T cells from seven different blood donors), in cultures containing the anti-OX40L specific neutralizing mAb 5A8. IL-2-activated NK cells that did not express OX40L were also able to costimulate the anti-CD3-induced proliferation of autologous CD4 T cells; however, this was always of a lower magnitude (approximately one third) than when the NK cells expressed OX40L as a consequence of prior stimulation via CD16 (Fig. 4*B*). An analysis of cytokines produced in these cultures revealed that the NK cell-costimulated T cells produced IFN- , but not IL-4 (Fig. 4*C*). Similar to the effects observed in the proliferation assays, anti-OX40L partially, but substantially, inhibited IFN- secretion induced by NK cell costimulation. In these experiments, fixed activated NK cells were used for costimulation to avoid the proliferation of the NK cells in response to IL-2, confirming that CD4 T cells were the responding population in the cultures, and to exclude that NK cell-derived cytokines were required for costimulation. We also established autologous NK:T cell cocultures with irradiated NK cells, and similar to fixed activated NK cells, irradiated activated NK also efficiently costimulated T cell proliferation in a OX40–OX40L dependent manner (data not shown).

Next, we investigated the role of OX40-OX40L interactions in autologous NK:T cell cocultures in response to a physiological TCR ligand, rather than anti-CD3 mAb. Bacterial superantigens bind with high affinity to MHC class II Ags on APCs and with TCR -chains on the responding T cells. This results in the T cell activation responsible for toxic shock syndrome and food poisoning. Activated NK cells express MHC class II molecules (36, 37) and present SEB to T lymphocytes (37). Thus, anti-CD16-activated MHC class II-positive NK cells and autologous freshly isolated resting CD4 T cells were cultured in the presence of different concentrations of SEB. As shown in Fig. 5*A*, activated NK cells efficiently present SEB to autologous CD4 T cells, stimulating T cell proliferation. Furthermore, OX40-OX40L interactions were required for optimal T cell proliferation, as shown in Fig. 5*B* by the ability of anti-OX40L mAb to substantially inhibit SEB-induced T cell proliferation. Collectively, these data indicate that CD16-activated NK cells can efficiently costimulate anti-CD3 or SEB-induced proliferation of autologous CD4 T cells, and that OX40L-OX40 interactions are critically involved.